

Journal Pre-proofs

Dihydropyridines as potential α -Amylase and α -Glucosidase Inhibitors: Synthesis, In Vitro and In Silico Studies

Hina Yousuf, Shahbaz Shamim, Khalid Mohammed Khan, Sridevi Chigurupati, Kanwal, Shehryar Hameed, Muhammad Naseem Khan, Muhammad Taha, Minhajul Arfeen

PII: S0045-2068(19)31311-2
DOI: <https://doi.org/10.1016/j.bioorg.2020.103581>
Reference: YBIOO 103581

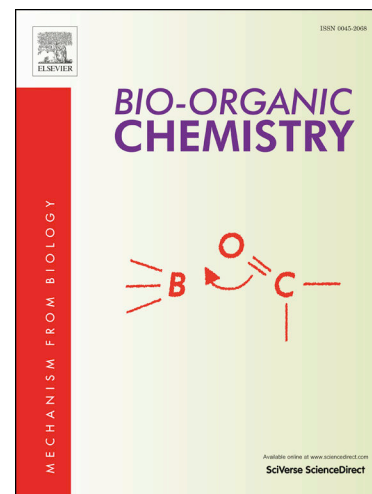
To appear in: *Bioorganic Chemistry*

Received Date: 9 August 2019
Revised Date: 30 November 2019
Accepted Date: 11 January 2020

Please cite this article as: H. Yousuf, S. Shamim, K. Mohammed Khan, S. Chigurupati, Kanwal, S. Hameed, M. Naseem Khan, M. Taha, M. Arfeen, Dihydropyridines as potential α -Amylase and α -Glucosidase Inhibitors: Synthesis, In Vitro and In Silico Studies, *Bioorganic Chemistry* (2020), doi: <https://doi.org/10.1016/j.bioorg.2020.103581>

This is a PDF file of an article that has undergone enhancements after acceptance, such as the addition of a cover page and metadata, and formatting for readability, but it is not yet the definitive version of record. This version will undergo additional copyediting, typesetting and review before it is published in its final form, but we are providing this version to give early visibility of the article. Please note that, during the production process, errors may be discovered which could affect the content, and all legal disclaimers that apply to the journal pertain.

© 2020 Published by Elsevier Inc.



Dihydropyridines as potential α -Amylase and α -Glucosidase Inhibitors: Synthesis, *In Vitro* and *In Silico* Studies

Hina Yousuf,^a Shahbaz Shamim,^a Khalid Mohammed Khan,^{a,b*} Sridevi Chigurupati,^c Kanwal,^a Shehryar Hameed,^a Muhammad Naseem Khan,^d Muhammad Taha,^b Minhajul Arfeen^c

^a*H. E. J. Research Institute of Chemistry, International Center for Chemical and Biological Sciences, University of Karachi, Karachi, 75270, Pakistan*

^b*Department of Clinical Pharmacy, Institute for Research and Medical Consultations (IRMC), Imam Abdulrahman Bin Faisal University, P.O. Box 1982, Dammam, 31441, Saudi Arabia*

^c*Department of Medicinal Chemistry and Pharmacognosy, College of Pharmacy, Qassim University, Buraidah, 52571, Saudi Arabia*

^d*Department of Chemistry, COMSATS University Islamabad, Abbottabad campus, Abbottabad (22010) Pakistan*

Abstract: Dihydropyridine derivatives **1-31** were synthesized *via* one-pot solvent free condition and screened for *in vitro* against α -amylase and α -glucosidase enzyme. The synthetic derivatives **1-31** showed good α -amylase inhibition in the range of $IC_{50} = 2.21 \pm 0.06 - 9.97 \pm 0.08 \mu\text{M}$, as compared to the standard drug acarbose ($IC_{50} = 2.01 \pm 0.1 \mu\text{M}$) and α -glucosidase inhibition in the range of $IC_{50} = 2.31 \pm 0.09 - 9.9 \pm 0.1 \mu\text{M}$ as compared to standard acarbose ($IC_{50} = 2.07 \pm 0.1 \mu\text{M}$), respectively. To determine the mode of binding interactions of synthetic molecules with active sites of enzyme, molecular docking studies were also performed. Different spectroscopic techniques such as ^1H -, ^{13}C -NMR, EI-MS, and HREI-MS were used to characterize all the synthetic compounds.

Keywords: Dihydropyridine; synthesis; α -amylase; α -glucosidase; *in vitro*; structure-activity relationship (SAR); *in silico* studies

Introduction

Heterocyclic chemistry have become very familiar in the pharmaceutical chemistry and organic synthesis. Additionally, science and technology are moving towards the environmental and economical caring, and supportable methods [1]. In the recent past the use of non-toxic and environment friendly reagents have attracted a great considerations of synthetic chemist to avoid the basic environmental toxins that have been harmful for the living organisms [2]. The solvent free one-pot multicomponent reactions are one of the basic approach in green chemistry

*Corresponding Authors: khalid.khan@iccs.edu, drkhalidhej@gmail.com, Tel.: +922134824910, Fax: +922134819018

to attain the desired products with minimal usage of harmful chemicals in short time and being economical [3]. The nitrogen containing heterocycles acquired much importance due to their role in biological systems. Dihydropyridines (DHPs) are a prolific source of pharmacological and biological actions. The 1,4-dihydropyridine nucleus is known as one of the most important heterocyclic framework that is found in many pharmaceuticals and drugs [2]. They are commercially used as calcium channel blocker [4].

Diabetes is a serious health disorder which in the 6th leading cause of global mortality and growing at alarming rates around the world [5]. Diabetes mellitus which is caused by deficient insulin secretion is known as type I DM, however, decrease utilization of insulin leads to type II DM [6]. Insulin is a peptide hormone that decreases blood glucose level by increased utilization of glucose thus reduces gluconeogenesis [7]. Type II diabetes is the most common form of diabetes, almost 80% to 90% of all the cases are suffered from this type [8].

α -Amylase is a common key enzyme found in pancreatic juice and saliva. α -Amylase effectively targets the control of postprandial hyperglycemia [9]. It acts randomly on internal α -1,4-glucosidic linkages of starch, glycogen, and related polysaccharides giving various kinds of oligosaccharides as end product. α -Amylase belongs to the family of glycoside hydrolases, and lies under glycoside hydrolases family 13. It can be isolated from different sources such as microbes, plants, and animals. Microbial amylases have advantages like space, cost and time effectiveness, and easy optimization of production process. Bacterial α -amylase can be easily engineered for the desired characteristics to enhance their industrial demands [10]. Unlike α -glucosidase that catalyses last step of disaccharides and starch hydrolysis, α -amylase involves in the hydrolysis of large starch molecules in to absorbable molecules. Therefore, it is an effective approach to inhibit pancreatic α -amylase to treat diabetes [9]. Acarbose, a tetrasaccharide mimic with potent α -amylase inhibitory activity is used to treat T2DM. Various α -amylase inhibitors have been isolated from nature and reported, however, selective and potent α -amylase inhibitors are still in search [7].

α -Glucosidase is present in the brush border surface membrane of the intestinal cells. It is one of the most important carbohydrate digestive enzyme [11]. It hydrolyzes the 1,4-linked α -glucose residues from the non-reducing end of polysaccharide to give a single α -glucose molecule. It performs an important role in the final step of carbohydrate digestion, therefore, inhibition of α -glucosidase can effectively control postprandial hyperglycemia. α -Glucosidase is also responsible for other diseases like viral infections and cancer [12]. Various α -glucosidase inhibitors such as acarbose, voglibose, and miglitol have been clinically approved.

These inhibitors are usually taken orally, acting as an antibiotic drug by delaying the absorption of sugar and suppressing the digestion of carbohydrate. It leads plasma glucose to be maintained at a steady level [13]. Unfortunately, α -glucosidase inhibitors cause flatulence, abdominal pain, diarrhea, and liver disorder which is most common in noncompliance. Therefore, research for finding new α -glucosidase inhibitors with minor or no side effects is an important task [14].

Our research group has identified many heterocyclic organic molecules of different classes in search for their potential uses in medicinal chemistry [15-20]. We have been working on the identification of small molecules that may act as lead compounds and may serve as potential antidiabetic agents. Nevertheless, recently we had designed, synthesized, identified, and reported dihydropyridine derivatives as potential α -glucosidase inhibitors [21] (Figure-1).

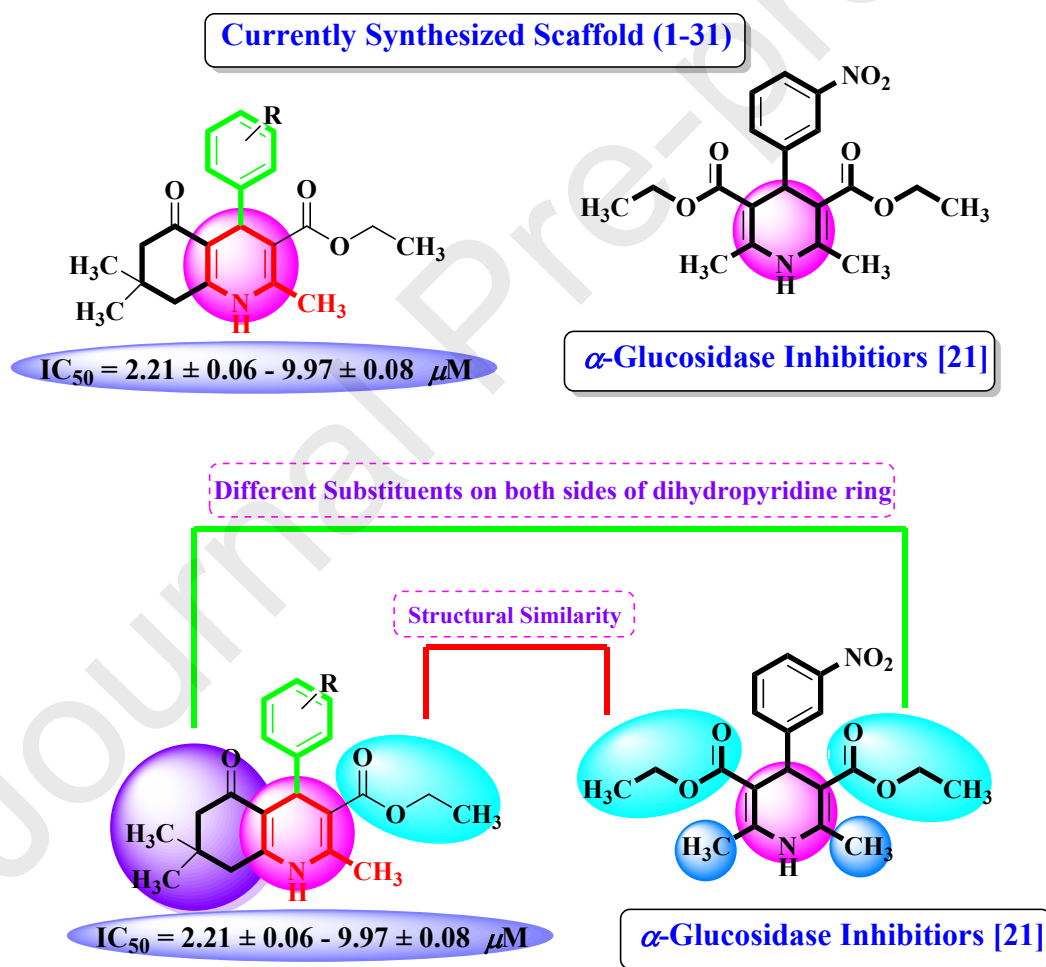


Figure-1: Rationale of the current study

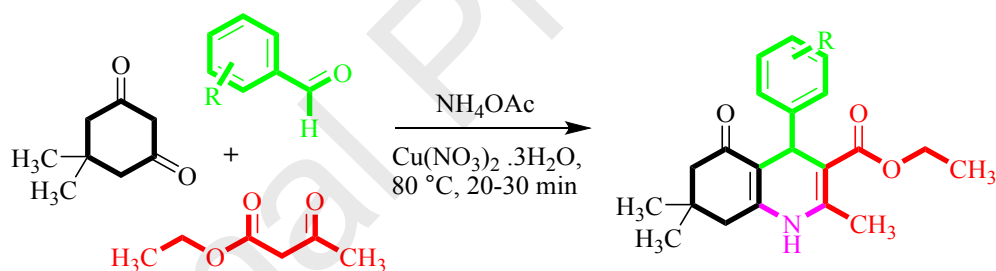
Keeping in mind the antidiabetic potential of dihydropyridines, synthesized compounds were also subjected for α -amylase and α -glucosidase inhibition. The synthetic compounds were structurally different from the previous compounds having two different substituents on either

side of dihydropyridine ring. The difference in structures resulted in better inhibitory action against α -amylase and α -glucosidase enzymes. Fortunately, we had identified dual and potential inhibitors of α -amylase and α -glucosidase enzymes that would be an ideal therapy for treatment of diabetes.

Results and Discussion

Chemistry

Ethyl-2,7,7-trimethyl-5-oxo-4-phenyl-1,4,5,6,7,8-hexahydroquinoline-3-carboxylate derivatives **1-31** were synthesized by reacting ethyl acetoacetate, dimedone, ammonium acetate, and different aryl aldehydes in “one pot”. The reaction was catalyzed with copper nitrate trihydrate ($\text{Cu}(\text{NO}_3)_2 \cdot 3\text{H}_2\text{O}$) in solvent free condition at 80-90 °C (Scheme-1). The reaction mixture was refluxed until a solid mass was obtained. Thin layer chromatography (TLC) was used to monitor the completion of reaction. After completion of reaction, the solid mass was filtered and washed with excess of distilled water followed by washing with hexane. Ethanol was used for crystallization to get pure products. Different spectroscopic techniques like ^1H -, ^{13}C -NMR, EI-MS, and HREI-MS were used to characterize the structures of synthetic compounds **1-31** (Table-1).



Scheme-1: Ethyl-2,7,7-trimethyl-5-oxo-4-phenyl-1,4,5,6,7,8-hexahydroquinoline-3-carboxylate derivatives (**1-31**)

***In vitro* α -amylase and α -glucosidase inhibitory activities:**

All synthetic ethyl-2,7,7-trimethyl-5-oxo-4-phenyl-1,4,5,6,7,8-hexahydroquinoline-3-carboxylate derivatives **1-31** were subjected for their *in vitro* α -amylase inhibitory activity. It is noteworthy that all synthetic compounds displayed good and moderate inhibitory activity against α -amylase with IC_{50} values in the range of 2.21 ± 0.06 - 9.97 ± 0.08 μ M and α -glucosidase in the range of $IC_{50} = 2.31 \pm 0.09$ - 9.9 ± 0.1 μ M as compared to the standard acarbose ($IC_{50} = 2.01 \pm 0.1$ μ M) (Table-1). The general structural features of the molecule comprise of pyrimidine ring, acetyl group, dimedone segment, and an aryl ring (R) (Figure-2). All these parts are playing important role in the activity, however, slight variation in the activity of synthetic molecules was might be due to variability in the positions and nature of substituents on ring (R).

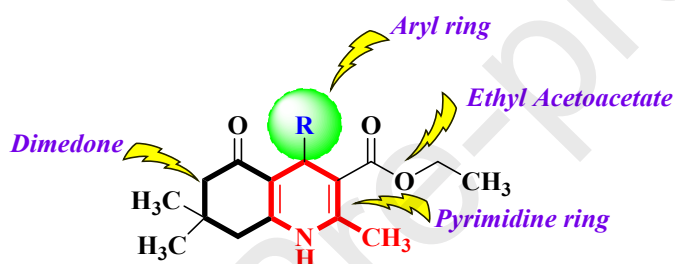
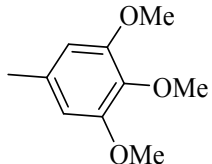
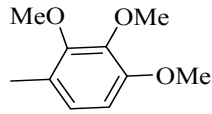
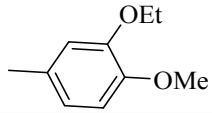
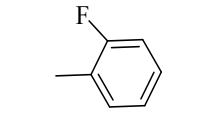
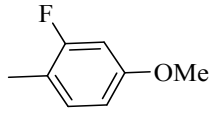
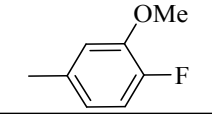
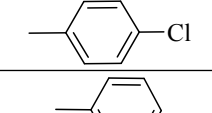
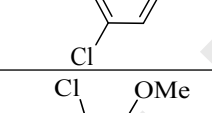
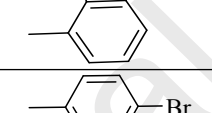
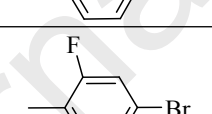
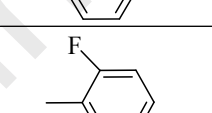
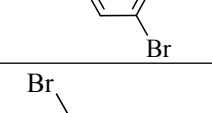
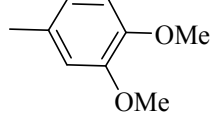
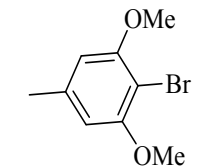
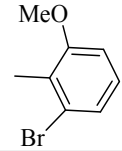
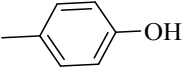
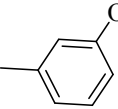
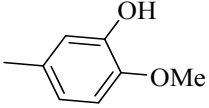
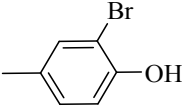
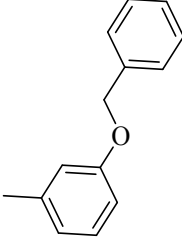
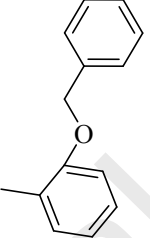
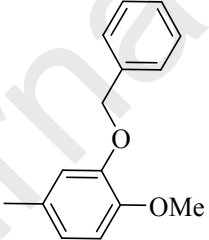
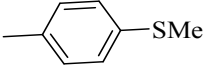
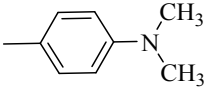
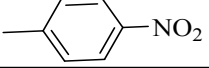
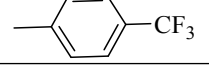


Figure-2: General structure of synthetic compounds

Table-1: *In vitro* α -amylase, α -glucosidase inhibitory activity of ethyl-2,7,7-trimethyl-5-oxo-4-phenyl-1,4,5,6,7,8-hexahydroquinoline-3-carboxylate derivatives (1-31)

Compounds No.	R	α -Amylase Inhibition $IC_{50} \pm SEM^a$ (μ M)	α -Glucosidase Inhibition $IC_{50} \pm SEM^a$ (μ M)
1		9.97 ± 0.08	9.9 ± 0.1
2		2.58 ± 0.09	2.88 ± 0.06
3		3.90 ± 0.18	4.01 ± 0.02
4		4.31 ± 0.3	4.82 ± 0.12
5		6.2 ± 0.03	6.4 ± 0.12

6		6.11 ± 0.12	6.17 ± 0.21
7		7.41 ± 0.12	7.71 ± 0.05
8		6.51 ± 0.13	6.9 ± 0.22
9		6.91 ± 0.12	7.31 ± 0.01
10		3.22 ± 0.05	3.02 ± 0.05
11		5.11 ± 0.23	5.22 ± 0.02
12		4.65 ± 0.08	4.95 ± 0.08
13		9.01 ± 0.14	9.14 ± 0.1
14		4.1 ± 0.11	4.22 ± 0.2
15		5.91 ± 0.03	5.92 ± 0.12
16		4.91 ± 0.13	4.95 ± 0.02
17		7.31 ± 0.12	7.61 ± 0.01
18		2.21 ± 0.06	2.31 ± 0.09
19		3.98 ± 0.08	3.08 ± 0.02

20		6.31 ± 0.13	6.44 ± 0.22
21		5.21 ± 0.3	5.42 ± 0.32
22		6.11 ± 0.13	6.14 ± 0.22
23		4.0 ± 0.18	4.08 ± 0.02
24		4.1 ± 0.11	4.22 ± 0.12
25		2.33 ± 0.05	2.55 ± 0.05
26		4.31 ± 0.03	4.55 ± 0.32
27		4.11 ± 0.13	4.9 ± 0.32
28		2.36 ± 0.1	2.77 ± 0.1
29		6.01 ± 0.13	6.34 ± 0.21
30		6.61 ± 0.23	7.01 ± 0.02
31		6.71 ± 0.11	7.11 ± 0.05
Acarbose (Standard)^b		$2.01 \pm 0.1-$	2.07 ± 0.1

SEM^a (Standard error of mean); Standard^b (Inhibitor for α -amylase, α -glucosidase enzymes).

Structure-Activity Relationship of α -Amylase Inhibitory Activity

All synthetic derivatives **1-31** were subjected for their *in vitro* α -amylase inhibitory activity. Limited structure-activity relationship was established based on variation in the substitution at ring "R". Compound **1** ($IC_{50} = 9.97 \pm 0.08 \mu M$) bearing benzene ring without any substitution displayed least activity amongst the series. Nevertheless, the substituted derivatives displayed good inhibitory activities in comparison with compound **1** showing that substitution on benzene ring increases the inhibitory potential of compounds. Among dimethoxy substituted derivatives, compound **2** ($IC_{50} = 2.58 \pm 0.09 \mu M$) with two methoxy groups *ortho* to each other showed similar activity to acarbose ($IC_{50} = 2.01 \pm 0.1 \mu M$). However, compounds **3** ($IC_{50} = 3.90 \pm 0.18 \mu M$) and **4** ($IC_{50} = 4.31 \pm 0.3 \mu M$) bearing two methoxy substituents *meta* to each other and compound **5** ($IC_{50} = 6.2 \pm 0.03 \mu M$) having two methoxy *para* to each other were found to be less active as compared to compound **2**. It showed that methoxy residues adjacent to each other displayed good α -amylase inhibitory activity and it may be capable to attain such conformation that will easily interact with enzyme. Among trimethoxy analogs, compounds **6** ($IC_{50} = 6.11 \pm 0.12 \mu M$) and **7** ($IC_{50} = 7.41 \pm 0.12 \mu M$) showed moderate activities as compared to the standard, might be the presence of the three methoxy groups resulted in increased steric hindrance thus having decrease interaction within enzyme's active site. Compound **8** ($IC_{50} = 6.51 \pm 0.13 \mu M$) possessing methoxy and ethoxy groups showed decreased activity in comparison with dimethoxy substituted compounds **2-5**, nonetheless, were more active than trimethoxy substituted compounds **6** and **7** (Figure-3).

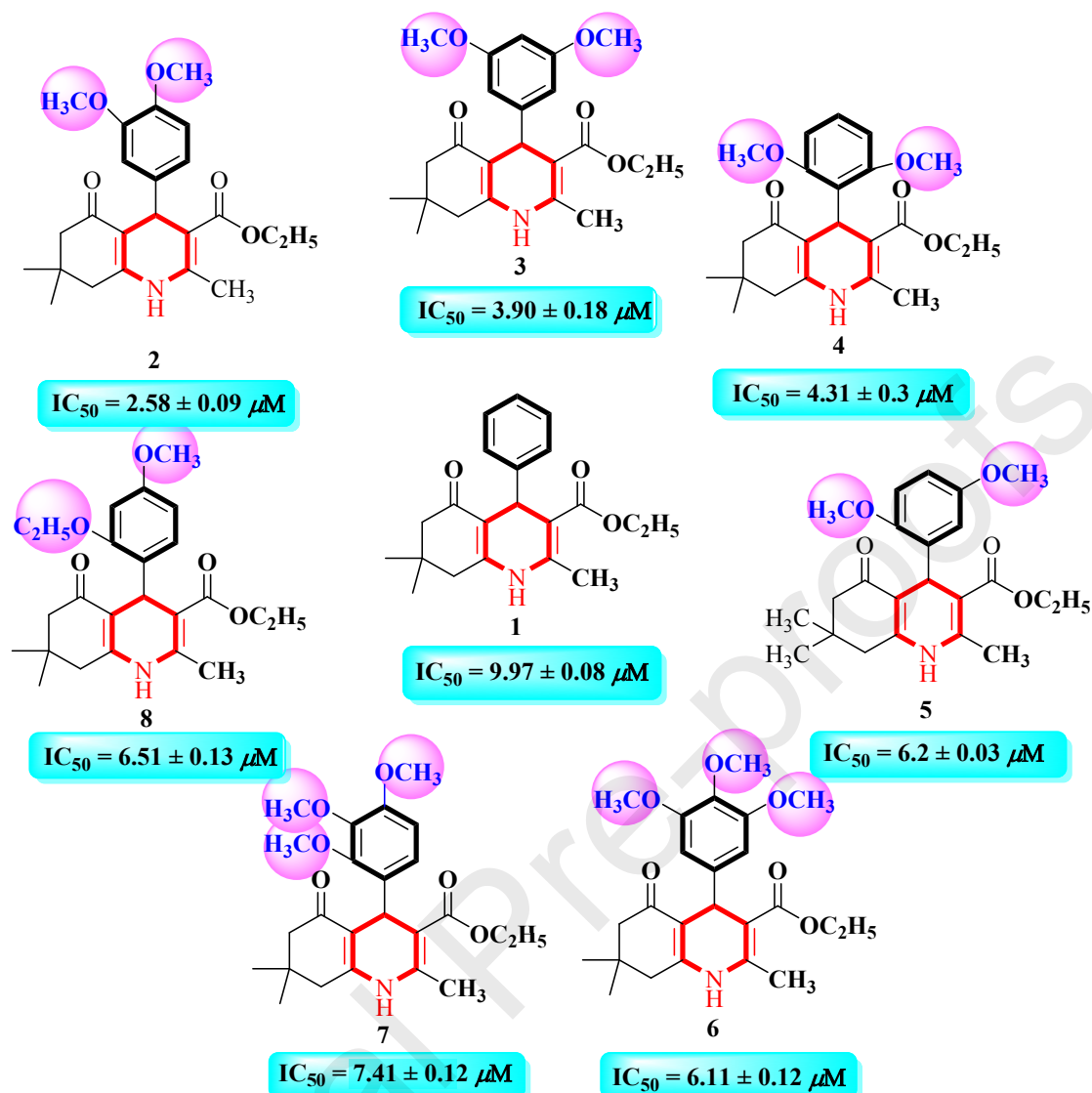


Figure-3: Structure-activity relationship of compounds 1-8

The halogen substituted compounds also showed good to moderate inhibitory activity. Compound 9 ($IC_{50} = 6.91 \pm 0.12 \mu M$) in which fluoro group is present at *ortho* position showed lesser activity. However, compound 12 ($IC_{50} = 4.65 \pm 0.08 \mu M$) bearing chloro substituent at *para* position was more active as compared to compound 13 ($IC_{50} = 9.01 \pm 0.14 \mu M$) with chloro group at *ortho* position. The chloro group at *ortho* position is near to side chain group might be creating steric hindrance thus results in reduced activity. The *para* bromo substituted compound 15 ($IC_{50} = 5.91 \pm 0.03 \mu M$) exhibited decreased activity as compared to chloro substituted analog 12. Compound 16 ($IC_{50} = 4.91 \pm 0.13 \mu M$) with addition of fluorine *meta* to bromine displayed enhanced activity, nevertheless, compound 17 ($IC_{50} = 7.31 \pm 0.12 \mu M$) with bromine and fluorine *para* to each other resulted in reduced activity. The reduced activity of compound 17 might be due to position of these two halogens on aryl ring (Figure-4).

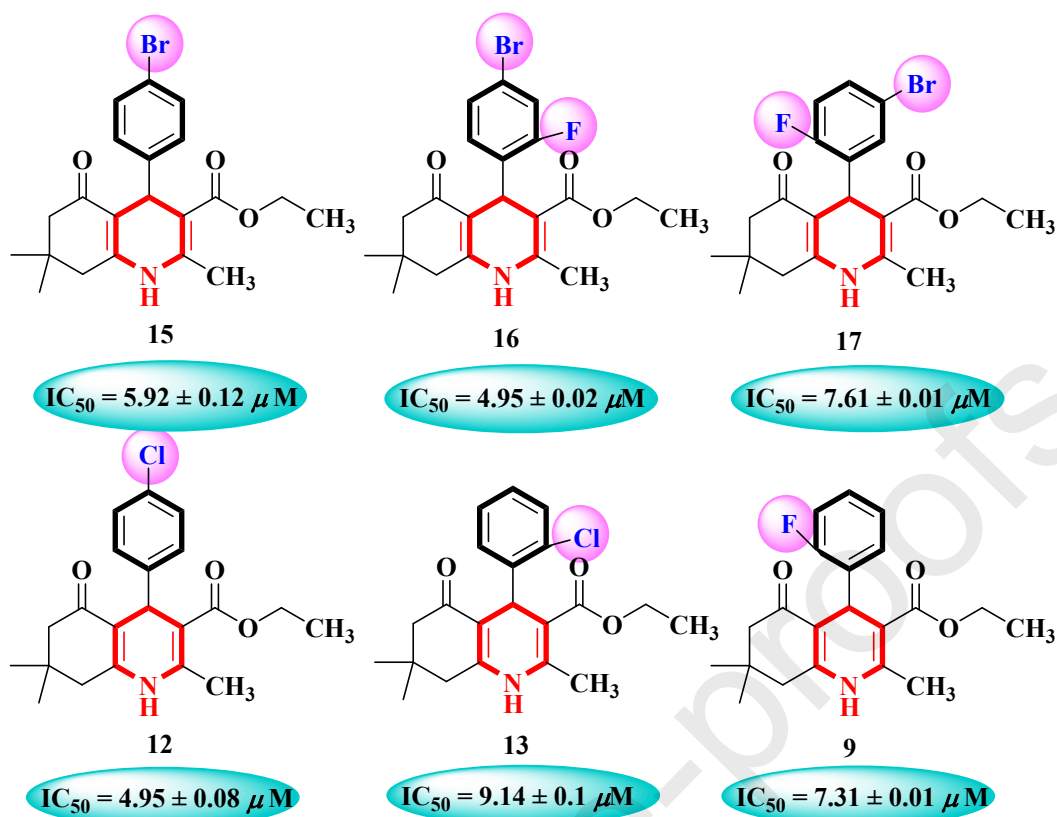


Figure-4: Structure-activity relationship of compounds 9, 12, 13, 15-17

The synthetic compounds with combination of methoxy and halogens also displayed good inhibition against α -amylase enzyme. The inhibitory potential of compound 9 might be compared with compounds 10 ($IC_{50} = 3.22 \pm 0.05 \mu M$) bearing fluoro and methoxy groups *para* to each other. Compound 10 displayed almost two folds increased inhibition might be the addition of methoxy group resulted in better interactions of compounds with the active site of enzyme. The change in positions of fluoro and methoxy groups in compound 11 ($IC_{50} = 5.11 \pm 0.23 \mu M$) resulted in decreased activity in comparison with compound 10, however, it is more active than compound 9. Compound 14 ($IC_{50} = 4.1 \pm 0.11 \mu M$) with addition of one methoxy group *ortho* to chlorine displayed enhanced activity in comparison with its other chloro substituted analogs. Compounds 18, 19, and 20 with the combination of bromo and methoxy groups displayed potent inhibitory activity. Compound 18 ($IC_{50} = 2.21 \pm 0.06 \mu M$) with bromo and two methoxy groups which are present at *meta* and *para* positions, respectively, displayed most activity among the whole library of compounds and activity of this compound might be due to better interaction of compound with enzyme. Compound 19 ($IC_{50} = 3.98 \pm 0.08 \mu M$) having a bromo in between two methoxy groups showed less activity than compound 18. However, compound 20 ($IC_{50} = 6.31 \pm 0.13 \mu M$) in which bromo and methoxy groups are

present *ortho* to each other displayed reduced activity which showed that position of bromo and methoxy groups displaying an important effect on the activity (Figure-5).

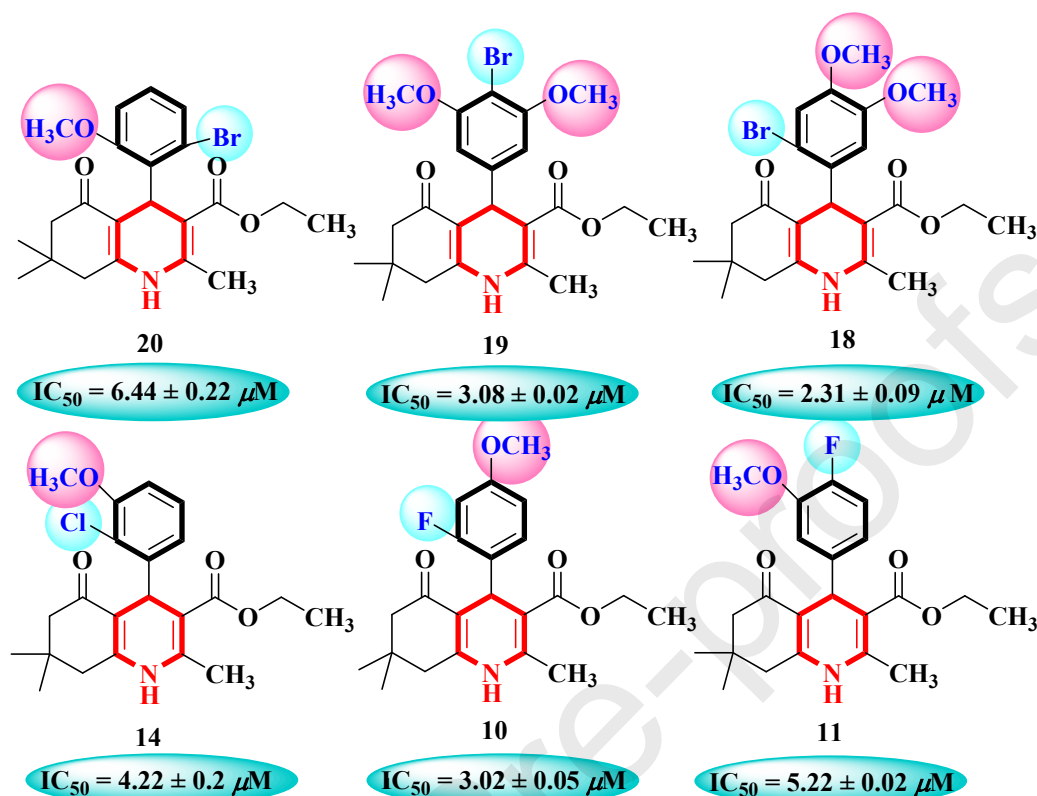


Figure-5: Structure-activity relationship of compounds 10, 11, 14, 18-20.

Compound **21** ($IC_{50} = 5.21 \pm 0.3 \mu M$) with hydroxy at *para* position showed moderate activity. Switching the position of hydroxy group from *para* to *meta* in compound **22** ($IC_{50} = 6.11 \pm 0.13 \mu M$) resulted in declined activity. Combination of other groups with hydroxyl displayed increased activity such as compound **23** ($IC_{50} = 4.0 \pm 0.18 \mu M$) having methoxy *ortho* to hydroxy group resulted in increased activity might be due to excessive hydrogen bonding of both polar groups within the active site of enzyme. Compound **23** displayed comparable activity with compound **24** ($IC_{50} = 4.1 \pm 0.11 \mu M$) having bromine *ortho* to hydroxy. Amongst the benzyloxy substituted molecules **25-27**, compound **25** ($IC_{50} = 2.33 \pm 0.05 \mu M$) in which benzyloxy is present at *meta* position showed two folds more potent activity than compounds **26** ($IC_{50} = 4.31 \pm 0.03 \mu M$) and **27** ($IC_{50} = 4.11 \pm 0.13 \mu M$) having benzyloxy present at *ortho* and *meta*, positions, respectively (Figure-6).

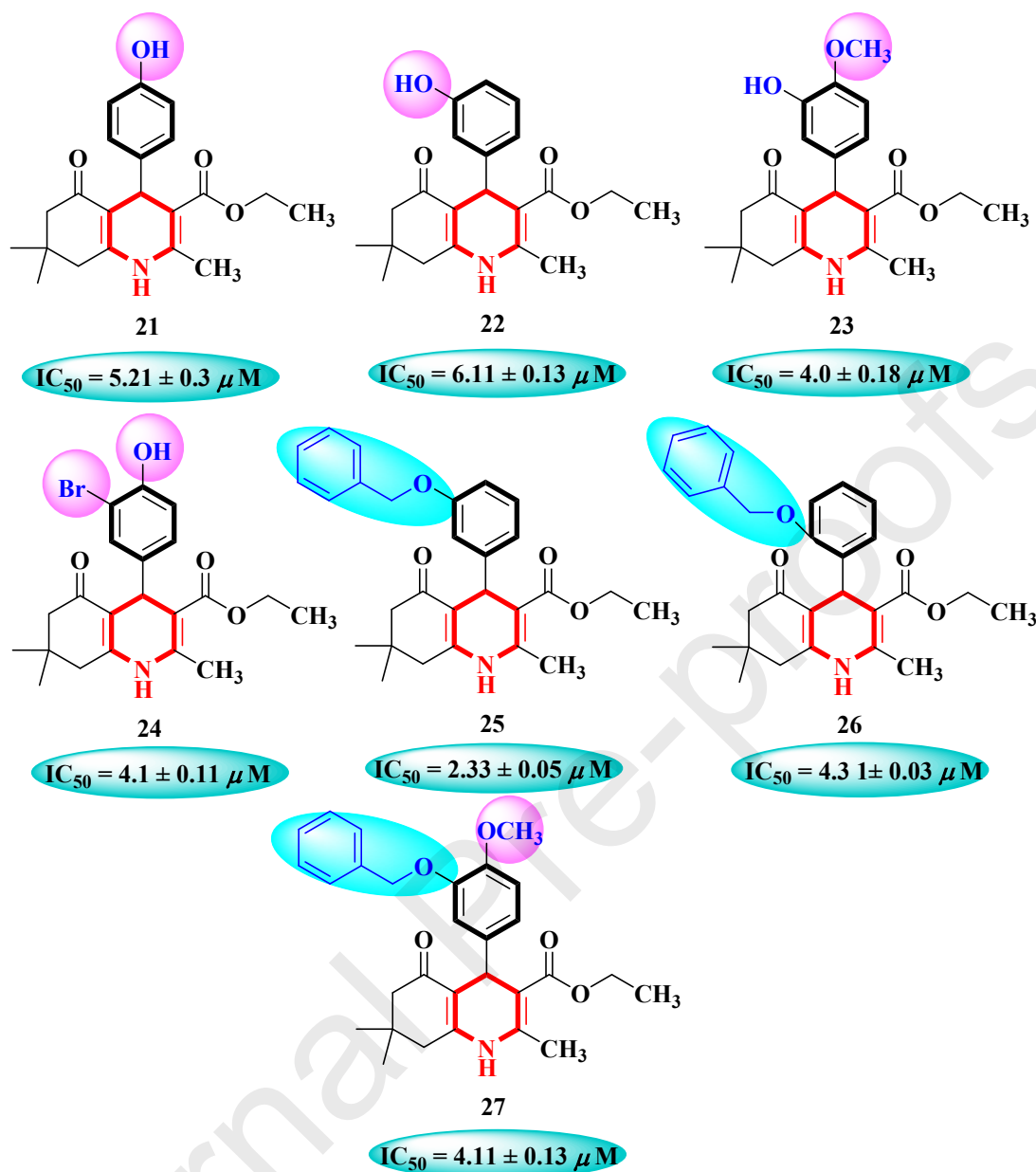


Figure-6: Structure-activity relationship of compounds 21-27

Compound **28** ($IC_{50} = 2.36 \pm 0.1 \mu M$) bearing a thiomethyl substitution displayed potent inhibition, the thiol group might have better interactions with the enzyme active site. Compound **29** ($IC_{50} = 6.01 \pm 0.13 \mu M$) with dimethyl amino group displayed moderate activity. Reduced activity might be due to steric hindrance by the two methyl groups on nitrogen. Compound **30** ($IC_{50} = 6.61 \pm 0.23 \mu M$) having nitro group showed further decreased activity might be due to electron withdrawing nature of nitro group. Compound **31** ($IC_{50} = 6.71 \pm 0.11 \mu M$) having trifluoro methyl substitution also displayed further decreased activity (Figure-7).

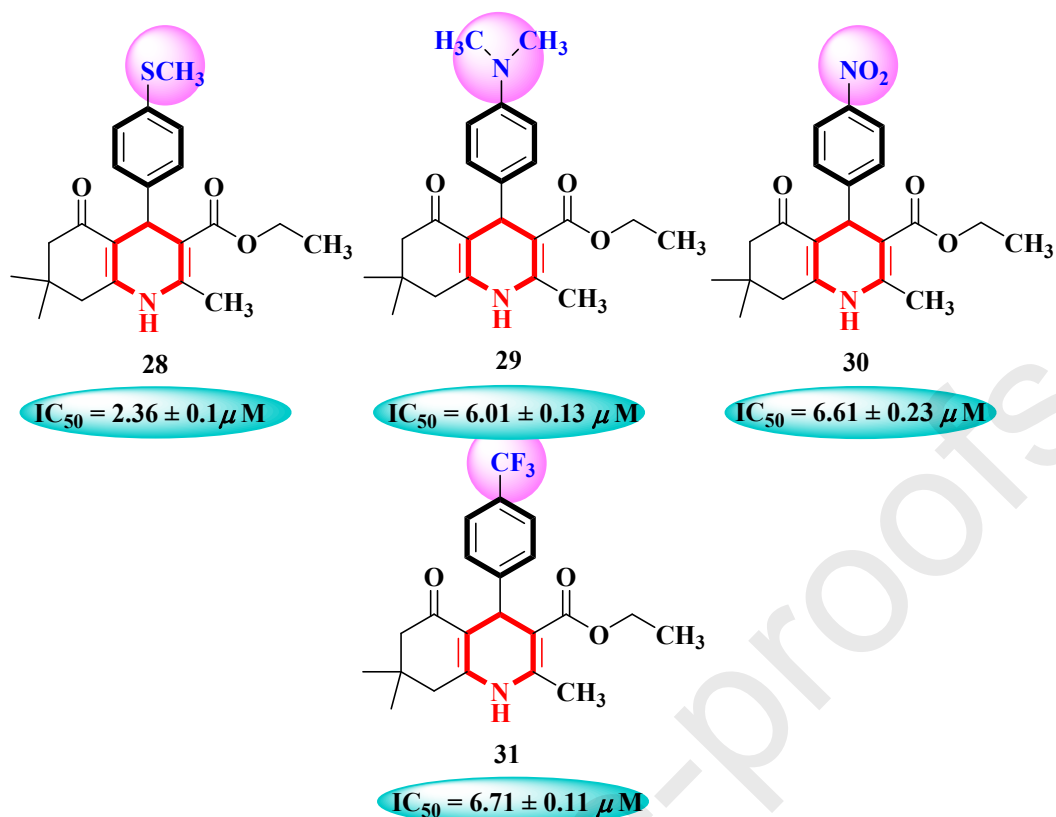


Figure-7: Structure activity relationship of compounds 28-31

Structure-Activity Relationship of α -Glucosidase Inhibitory Activity

All synthetic derivatives 1-31 exhibited good to moderate α -glucosidase inhibitory activity in the range of $IC_{50} = 2.31 \pm 0.09 - 9.9 \pm 0.1 \mu M$ as compared to the standard acarbose $IC_{50} = 2.07 \pm 0.1 \mu M$. Compound 1 ($IC_{50} = 9.9 \pm 0.1 \mu M$) with unsubstituted benzene ring displayed least activity among all compounds of the library. Among dimethoxy substituted derivatives, compound 2 ($IC_{50} = 2.88 \pm 0.06 \mu M$) bearing two methoxy groups which are present *ortho* to each other showed good inhibitory potential and was found to be more active in comparison with compounds 3 ($IC_{50} = 4.01 \pm 0.02 \mu M$) and 4 ($IC_{50} = 4.82 \pm 0.12 \mu M$) bearing two methoxy groups *meta* to each other. Nevertheless, compound 5 ($IC_{50} = 6.4 \pm 0.12 \mu M$) having two methoxy groups *para* to each other was least active amongst di methoxy substituted compounds. Compound 8 ($IC_{50} = 6.9 \pm 0.22 \mu M$) bearing methoxy and ethoxy groups *ortho* to each other was less active in comparison with compound 2 which suggests that methoxy groups at *ortho* positions are actively participating in the activity (Figure-8).

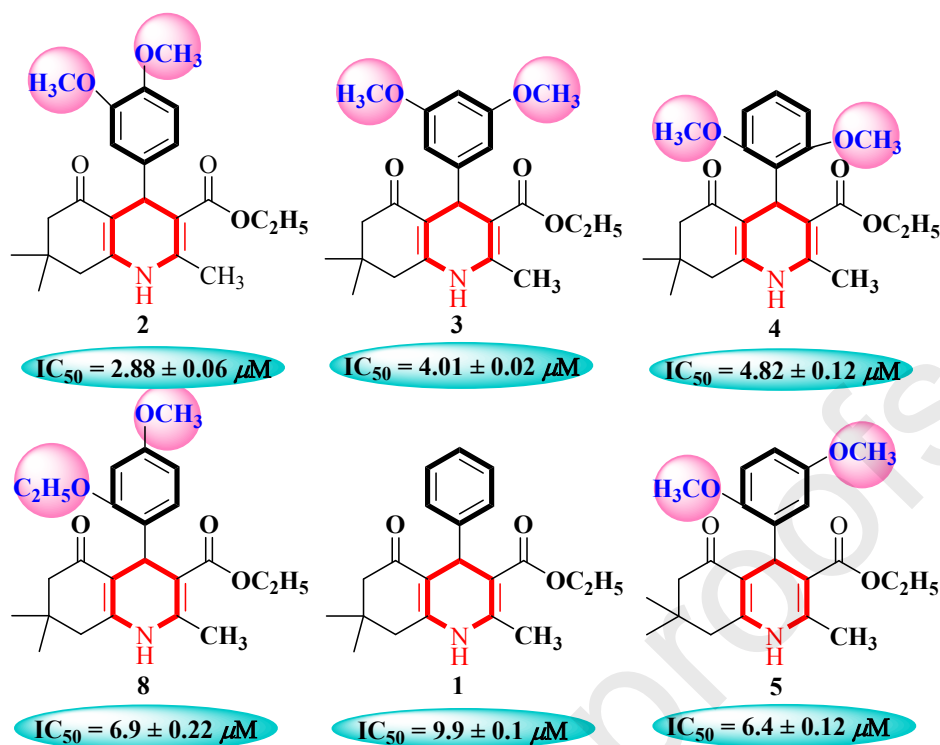


Figure-8: Structure-activity relationship of compounds 1-5, 8

The trimethoxy substituted compounds were less active than dimethoxy compounds. Among trimethoxy substituted derivatives, compound **6** ($IC_{50} = 6.17 \pm 0.21 \mu M$) was more active than compound **7** ($IC_{50} = 7.71 \pm 0.05 \mu M$), since in compound **7** three methoxy groups were adjacent to the bulky group of benzene ring so it increases hindrance and decreases chance of binding with active site of enzyme, therefore, the activity was decreased (Figure-9).

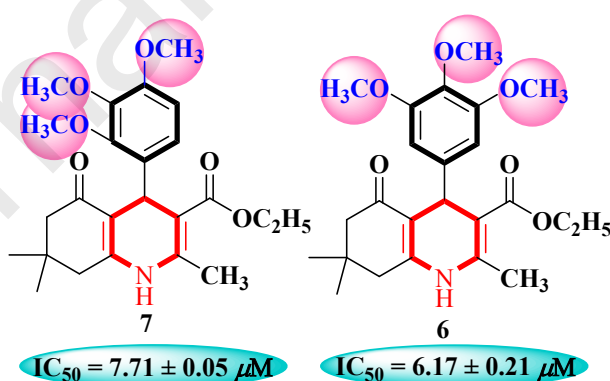


Figure-9: Structure-activity relationship of compounds 6-7

Compound **9** ($IC_{50} = 7.31 \pm 0.01 \mu M$) with fluoro group exhibited weak inhibitory potential as compared to the standard acarbose. Among chloro substituted derivatives, compound **12** ($IC_{50} = 4.95 \pm 0.08 \mu M$) bearing chloro group at *para* position was two folds more active than *ortho* chloro substituted compound **13** ($IC_{50} = 9.14 \pm 0.1 \mu M$). Compound **15** ($IC_{50} = 5.92 \pm 0.1 \mu M$) with *para* substituted bromo group also exhibited decreased activity as compared to chloro

substituted compound **12**. Compound **16** ($IC_{50} = 4.95 \pm 0.02 \mu\text{M}$) bearing bromo and fluoro substituents *meta* to each other was more active as compared to compound **17** ($IC_{50} = 7.61 \pm 0.01 \mu\text{M}$) in which bromo and fluoro groups were *para* to each other (Figure-10).

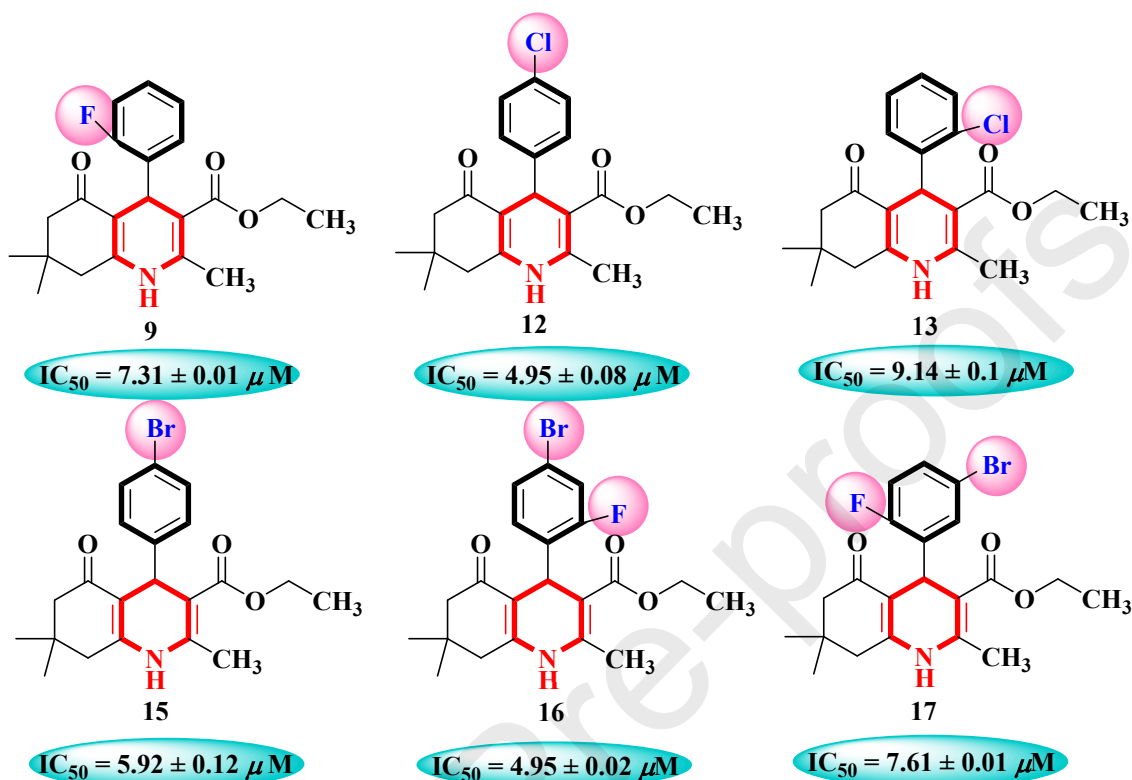


Figure-10: Structure-activity relationship of compounds 9, 12-17

Compounds **10** ($IC_{50} = 3.02 \pm 0.05 \mu\text{M}$) and **11** ($IC_{50} = 5.22 \pm 0.02 \mu\text{M}$) bearing methoxy groups that are present *meta* and *ortho* to fluoro, respectively, displayed good inhibitory activity in comparison with mono fluoro substituted compound **9**. The combination of chloro with methoxy also exhibited enhanced activity in compound **14** ($IC_{50} = 4.22 \pm 0.2 \mu\text{M}$) as compared to its chloro substituted derivatives. Compound **18** ($IC_{50} = 2.31 \pm 0.09 \mu\text{M}$) having bromo and two methoxy groups was most potent compound of this series and it displayed comparable activity with the standard acarbose ($IC_{50} = 2.07 \pm 0.1 \mu\text{M}$). However, changing the positions of bromo and methoxy groups in compound **19** ($IC_{50} = 3.08 \pm 0.02 \mu\text{M}$) resulted in decreased activity. Compound **20** ($IC_{50} = 6.44 \pm 0.22 \mu\text{M}$) with one methoxy group along with bromo showed less activity than compound **18** and **19**. It was observed that addition of methoxy with bromo displayed increased activity (Figure-11).

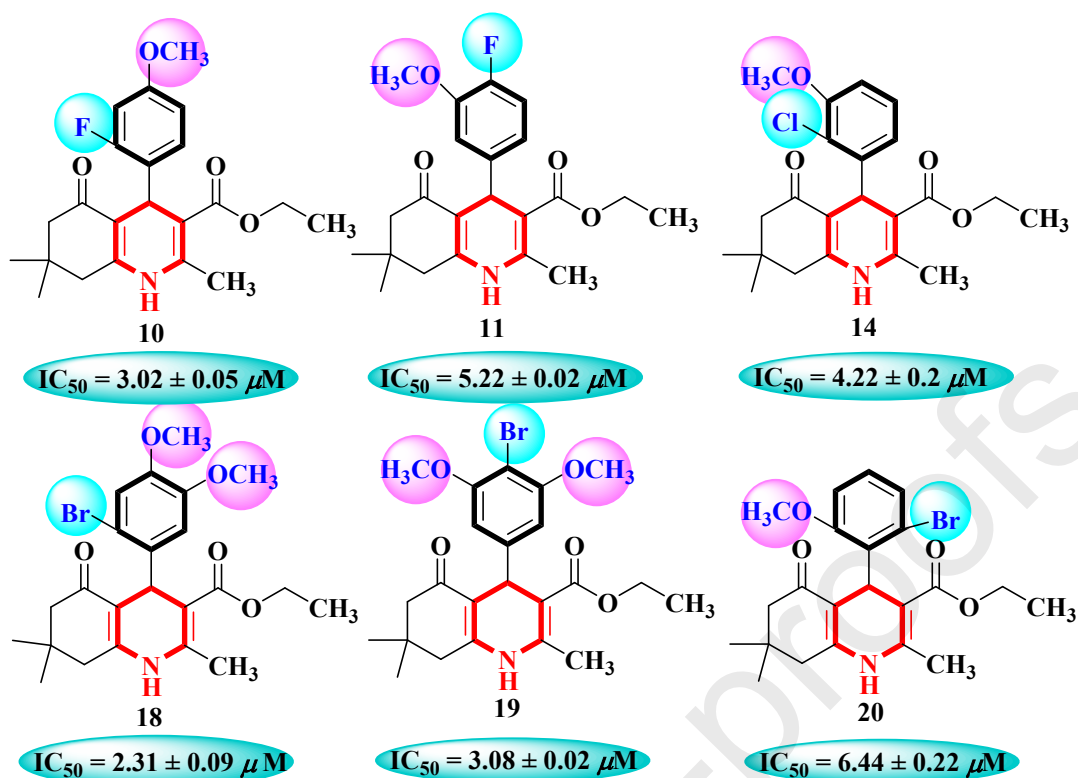


Figure-11: Structure-activity relationship of compounds 10, 11, 14, 18-20

Among mono hydroxy substituted derivatives, compound **21** ($IC_{50} = 5.42 \pm 0.32 \mu M$) with *para* substitution showed more activity as compared to compound **22** ($IC_{50} = 6.14 \pm 0.22 \mu M$) having *meta* substitution. It was found that hydroxy substitution at *meta* is creating hindrance with bulky group of benzene thus it will not easily attain such conformation which will interact well with enzyme. Compound **23** ($IC_{50} = 4.08 \pm 0.02 \mu M$) in which methoxy group was present *ortho* to hydroxy exhibited increased activity as compared to compound **24** ($IC_{50} = 4.22 \pm 0.12 \mu M$) bearing bromo group *ortho* to hydroxy group. Compound **25** ($IC_{50} = 2.55 \pm 0.05 \mu M$) having benzyloxy group at *meta* position displayed potential inhibitory activity. Shifting of benzyloxy group from *meta* to *ortho* showed decreased activity in compound **26** ($IC_{50} = 4.55 \pm 0.32 \mu M$) because bulky benzyloxy at *ortho* position creates more hindrance with another bulky group of benzene ring so it will not easily interact with active site of enzyme. Compound **27** ($IC_{50} = 4.9 \pm 0.32 \mu M$) in which methoxy group was added *ortho* to benzyloxy group exhibited further decreased activity (Figure-12).

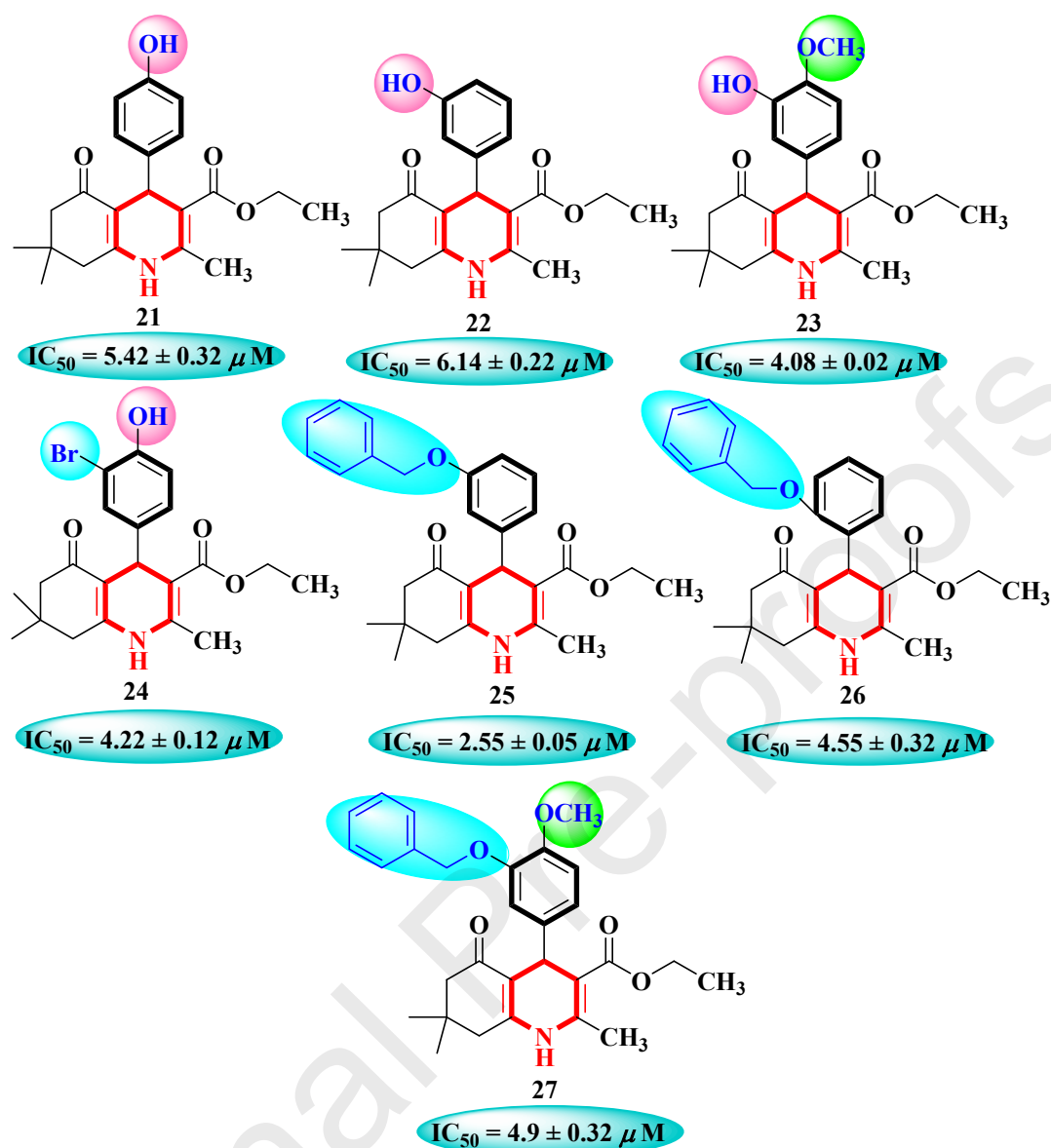


Figure-12: Structure-activity relationship of compounds 21-27

Compound **28** ($IC_{50} = 2.77 \pm 0.1 \mu M$) with *para* thiomethyl substitution displayed good activity as compared to the standard acarbose. Compound **29** ($IC_{50} = 6.34 \pm 0.21 \mu M$) having dimethyl amino substitution showed decreased activity as compared to compound **28**. Compound **30** ($IC_{50} = 7.01 \pm 0.02 \mu M$) with nitro group was found to be moderately active might be due to electron withdrawing effect of nitro group. Compound **31** ($IC_{50} = 7.11 \pm 0.05 \mu M$) bearing trifluoromethyl substitution displayed weak inhibitory potential (Figure-13).

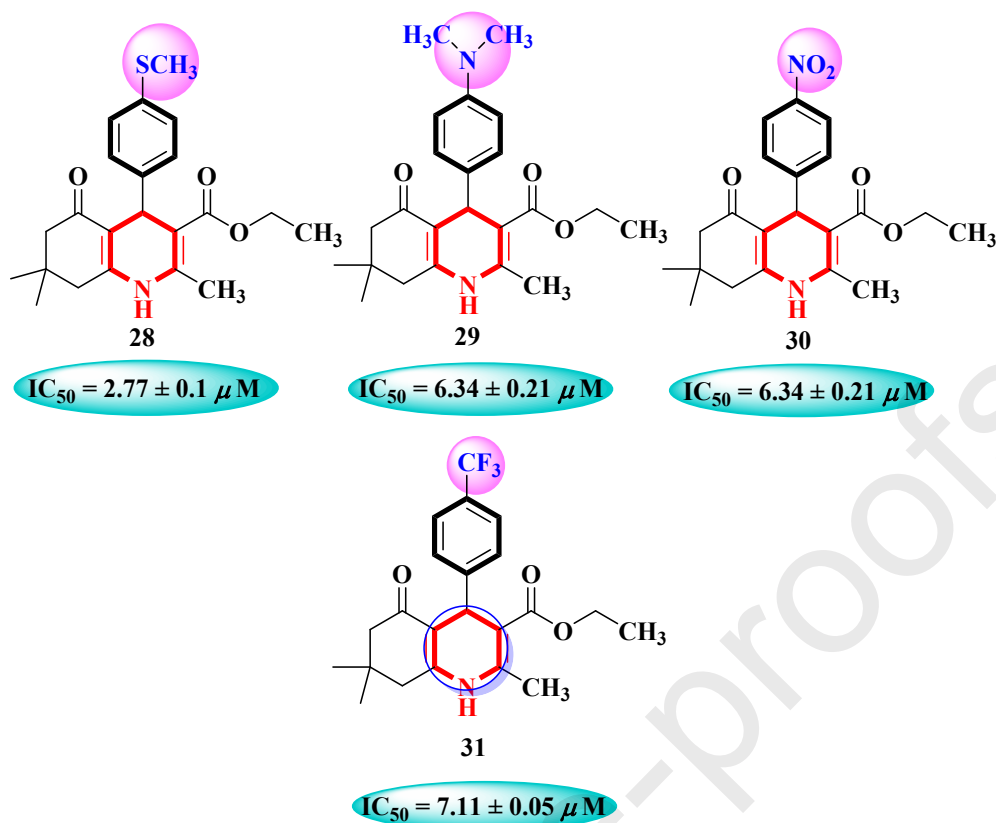


Figure-13: Structure-activity relationship of compounds 28-31

2.3. Docking studies

In present study, molecular docking studies were carried out using Autodock Vina for **1-31** synthetic compounds against α -amylase and α -glucosidase by targeting their active sites and investigating the binding poses adopted by the ligands. The docking parameters for α -amylase were validated by re-docking acarbose in the binding site of crystallographic protein (PDB ID: 3BAJ) with same parameters as used for the docking of synthesized ligands in the active site of α -amylase. As shown in **Figure-14**, the re-docked (blue) acarbose showed interaction in almost similar manner like its matching crystallographic conformation (red), declaring the selected parameters to be acceptable. While, the Autodock Vina parameters selected for α -glucosidase were verified in our previous study.

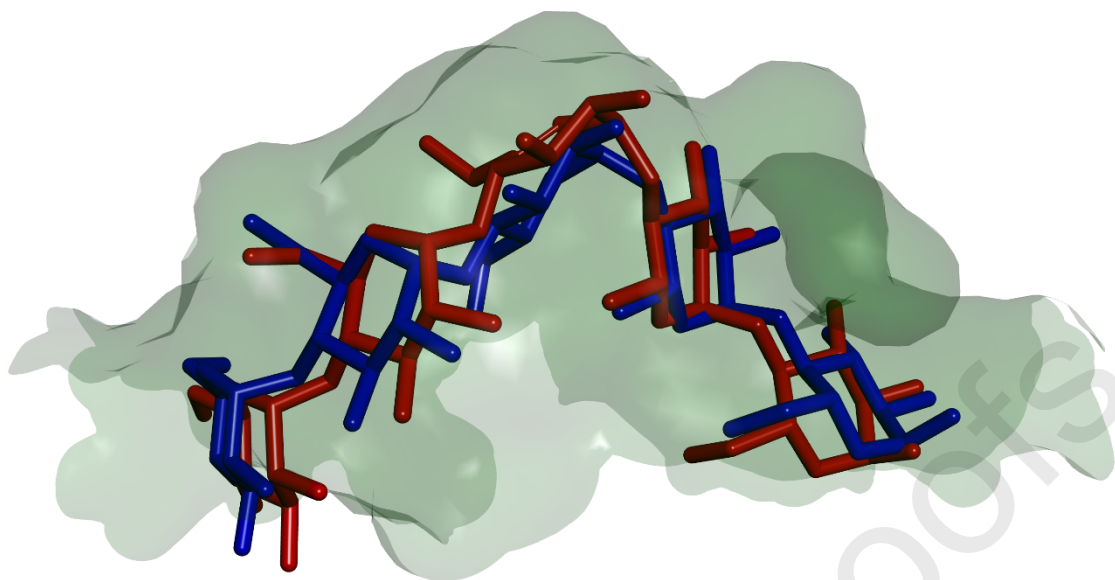


Figure-14: Overlap of re-docked (blue) and crystallographic (red) conformations of acarbose in α -amylase (3BAJ).

Study carried out with α -amylase displayed significant interactions between the synthesized ligands and side chain amino acids of the active site *i.e.* Ala198, Lys200, His201, Trp58, Trp59, Tyr151, Asp197, Glu233, Leu162, Thr163, Arg195, and Asp300. These are the most active compounds of the series *i.e.* **18**, **25**, **28**, and **2** displayed numerous strong interactions through residues which are present on side chain of the active site of α -amylase. Compound **18** ($IC_{50} = 2.21 \pm 0.06 \mu\text{M}$) (**Figure-15a**) which is the most active compound, its graphical investigation displayed that oxygen atom of ketonic group mediated a hydrogen bond interaction with side chain imidazole -NH of His305 (3.00 Å), however, the bromine atom at *ortho* position of phenyl group was found making hydrogen bond interaction with the hydroxyl group of side chain Thr163 (3.26 Å). Sidewise, following three carbon hydrogen bond interactions were spotted between the docked ligand and the side chain residues of the active site; **i**) between *para* substituted methoxy of phenyl ring and hydroxyl group of side chain Tyr151 (3.54 Å), **ii**) between alkyl chain of ester group and carboxylate group of side chain Glu233 (3.51 Å) and **iii**) between *meta* substituted methoxy group and carboxylate group of side chain Asp300 (3.01 Å), respectively. Other interactions which were associated in stabilization of the complex were the alkyl interaction between bromine atom of phenyl group and side chain Leu162 and π -sigma interactions between the methyl groups of **18** and indole rings of Trp59.

Binding manner of **25**, which displayed as second most active derivative ($IC_{50} = 2.33 \pm 0.05 \mu\text{M}$) revealed this compound was involved in forming almost the same interactions as that formed by **18** including one hydrogen bond interaction between ketonic group of quinoline and

side chain imidazole-NH of His305 (3.05 Å) as shown in **Figure-15b**. Whilst, the second hydrogen bond formed by the bromine atom of compound **18** and side chain Thr163 was not found in this case. Although, the phenyl ring of benzyloxy group was found in forming numerous interactions including π -anion, π -sigma, π - π T-Shaped and π -alkyl interactions with the side chain Glu233, Ile235, His201, Lys200 and Ala198, respectively. These interactions could be the main reason for stabilizing the ligand receptor complex and making the derivative second most active analog among the series.

The binding manner of another active molecule of the series, compound **28** ($IC_{50} = 2.33 \pm 0.05 \mu\text{M}$) (**Figure-15c**) displayed that this compound was found in forming a single strong hydrogen bond interaction between the NH group of quinoline and the carboxylate oxygen atom of side chain Asp300 (2.19 Å). A carbon hydrogen bond which was found between the ethyl group of ester and carbonyl oxygen of side chain of Tyr62 showed a bond distance of 3.71 Å. Other interactions which could be resulting in decreasing the energy of the complex were the π -sulfur and π -sigma interactions between the methylthio group of compound **28** and the indole ring of side chain Trp59 and alkyl interactions between the methyl group of ligand and alkyl part of side chain Ile235.

Docking results of fourth most active analog of the series, compound **2** ($IC_{50} = 2.58 \pm 0.09 \mu\text{M}$) displayed its involvement in formation of two hydrogen bond interactions between the oxygen atom of ester group and side chain imidazole-NH of His305 (3.13 Å) and between carbonyl oxygen of ketonic group and hydroxyl group of side chain Thr163 (2.73 Å), respectively (**Figure-15d**). Also, a carbon hydrogen bond of 3.65 Å was found between the methoxy group at *para* position of phenyl ring and carboxylate oxygen which is present on side chain Asp300. Among hydrophobic interactions, the two methyl groups of this compound were also mediating a π -alkyl interaction with the side chain Trp59.

Ultimately, in the docking study of α -amylase inhibition, the interactions of least active compounds *i.e.* **13** ($IC_{50} = 9.01 \pm 0.14 \mu\text{M}$) and **1** ($IC_{50} = 9.97 \pm 0.08 \mu\text{M}$) were also analyzed and it was found that these two compounds failed to develop hydrogen bond interactions with the residues of the active site (**Figure-15e** and **Figure-15f**). Furthermore, compound **13** bearing chlorine atom at *ortho* position resulted in making more hydrophobic interactions with the amino acids which are present on the side chain of the active site as compared to **1**. Therefore, the phenyl ring substitution greatly influenced the interaction of ligands and the active site residues. Although, the substituted phenyl ring itself was not involved in making important

interactions with catalytic residues but it resulted the parent molecule to interact and make stronger interactions with the catalytic residues.

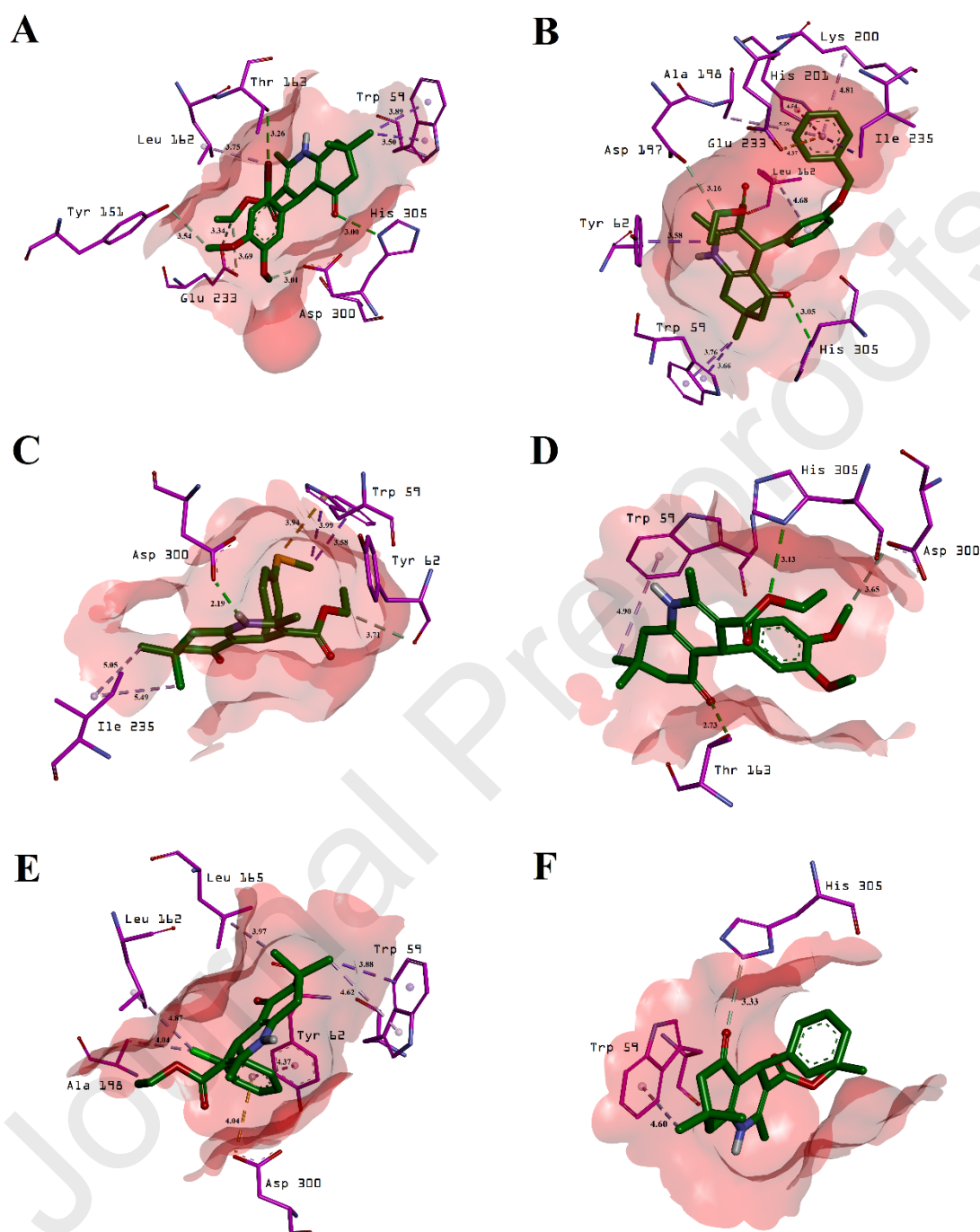


Figure-15: Docked conformation of synthesized compounds with the side chain residues of α -amylase, Ligands shown in green color, side chain amino acids in violet color, and distances (Angstrom) colored in black; A) Interactions of compound **18**; B) Interactions of compound **25**; C) Interactions of compound **28**; D) Interactions of compound **2**; E) Interactions of compound **13** and F) Interactions of compound **1**.

Molecular docking studies was also performed to support the *in vitro* inhibition potential studies of synthetic derivatives against α -glucosidase in which Autodock Vina is used. All

synthetic compounds were docked against established homology model of α -glucosidase. The most active molecule of the series showed significant interactions with the side chain amino acids of the homology modeled α -glucosidase. The most active compound **18** (**Figure-16a**) was found in establishing three hydrogen bond interactions with the side chain residues of the active site *i.e.* **i**) between carbonyl oxygen of ester group and NH group of side chain Asn241 (1.78 Å), **ii**) between oxygen of ethoxy group and the side chain imidazole-NH of His279 (2.33 Å) and **iii**) between carbonyl oxygen of ketonic group and side chain NH groups of Arg312 (1.95 Å and 2.64 Å), respectively. Other residues which were found in making hydrophobic interactions with compound **18** were the involvement of Phe157, Pro309 and Phe310 in forming carbon hydrogen bonds, Phe157 and Phe300 forming π -alkyl interactions and Glu304 spotted in creating halogen bonding with the bromine atom which is present at *ortho* position. The predicted binding modes of compound **25** which is the second most active compound in the whole series displayed that the compound was involved in various interactions as shown in **Figure-16b**. The carbonyl oxygen of ketonic group was found in developing two hydrogen bond interactions with the NH groups of side chain Arg312 with the bond distances of 2.43 Å and 2.47 Å, respectively. While, the carbonyl group of the ester was found in forming hydrogen bond interaction with the NH group of side chain His279 (2.00 Å). Other interactions which could have resulted in stabilizing the ligand receptor complex are the formation of hydrophobic interactions which are found between the ligand and side chain residues including Phe157, Phe177, Pro240 and Arg312, respectively.

The third and fourth most active compounds **28** and **2** (**Figure-16c** and **Figure-16d**) were also involved in forming hydrogen bond interactions with side chain amino acids of the active site. The carbonyl oxygen of compound **28** was found forming two hydrogen bonds with the NH groups of side chain Arg312 having a bond distance of 2.75 Å and 2.76 Å, respectively. While, compound **2** was found forming three hydrogen bond interactions *i.e.* **i**) between methoxy oxygen at *para* position and NH group of side chain His239 (2.33 Å), **ii**) between ethoxy oxygen of ester group and NH group of side chain His279 (2.14 Å) and **iii**) between carbonyl oxygen of ester group and NH group of side chain Arg312 (2.82 Å), respectively. Meanwhile, the sulfur atom of compound **28** was also found in forming π -sulfur interaction with the phenyl ring of side chain Phe311. Other interactions resulting in minimizing the energy of the complex formed by compound **28** and **2** were the carbon hydrogen interactions of the ethyl chains of the ester group of both compounds with the side chain Glu304 and hydrophobic interactions

including alkyl-alkyl interactions, π -alkyl interactions and π -sigma interactions with the side chain residues including Lys155, Phe158, Phe177, and Phe300, respectively.

The least active derivatives among the series were also analyzed by studying their predicted binding modes as shown in **Figure-16e** and **Figure-16f**. Both compound **13** and **1** were found forming less interactions with the residues of active site as those formed by the active compounds. Compound **13** was found in forming interactions with only four residues of the active site including one hydrogen bond interaction between the carbonyl oxygen of ester group and NH group of side chain His239 (2.78 Å). While, compound **1** was also found in forming a single hydrogen bond interaction between the NH group of quinoline and carbonyl oxygen of side chain Phe157 (1.82 Å). Although, these compounds show inhibitory potential, but their least activeness as compared to the most active compounds of the series may be due to the establishment of less interactions with the active site of the enzyme. Therefore, it is concluded that those derivatives which contained substituents which are present on the *meta* and *para* position of the substituted phenyl ring resulted the docked complex to form more interactions as compared to those derivatives which contained either no substitution or were *ortho* substituted.

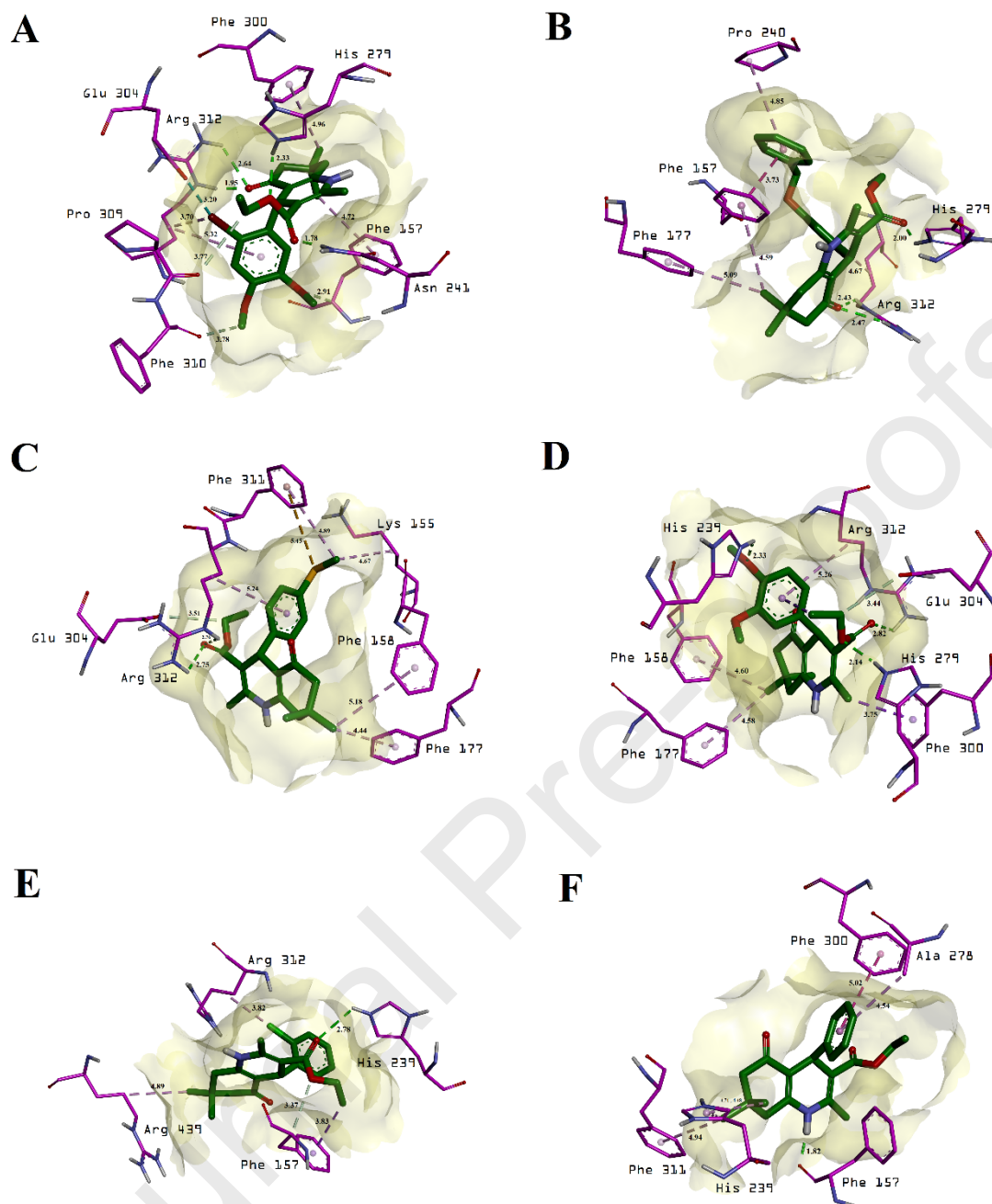


Figure-16: Docked conformation of synthesized compounds with the side chain residues of α -glucosidase, Ligands shown in green color, side chain amino acids in violet color, and distances (Angstrom) colored in black; A) Interactions of compound **18**; B) Interactions of compound **25**; C) Interactions of compound **28**; D) Interactions of compound **2**; E) Interactions of compound **13** and F) Interactions of compound **1**.

Conclusion

Ethyl-2,7,7-trimethyl-5-oxo-4-phenyl-1,4,5,6,7,8-hexahydroquinoline-3-carboxylates (**1-31**) were synthesized and evaluated for their antidiabetic potential. The synthetic molecules were subjected for their *in vitro* α -amylase and α -glucosidase inhibitory activities and displayed

potential inhibition against α -amylase in the range of ($IC_{50} = 2.21 \pm 0.06 - 9.97 \pm 0.08 \mu\text{M}$) as compared to the standard acarbose ($IC_{50} = 2.01 \pm 0.1 \mu\text{M}$). The synthetic derivatives also exhibited good to moderate α -glucosidase inhibition in the range of ($IC_{50} = 2.01 \pm 0.1 - 2.31 \pm 0.09 - 9.9 \pm 0.1 \mu\text{M}$) as compared to the standard acarbose ($IC_{50} = 2.07 \pm 0.1 \mu\text{M}$). Limited structure-activity relationship deduced that almost all structural features are contributing in the α -amylase and α -glucosidase inhibition, however, compounds with functional groups such as F, Cl, Br, OH, and OMe were actively participating in the activity. To identify the structural features that were involved in the binding interactions with the active site of enzyme *in silico* study was also performed. This study has showed various chemical spaces that may be use as lead molecules for future research to discover good α -amylase and α -glucosidase inhibitors for the treatment of diabetes patients.

Experimental

General procedure for the synthesis of Ethyl-2,7,7-trimethyl-5-oxo-4-phenyl-1,4,5,6,7,8-hexahydroquinoline-3-carboxylate derivatives (1-31)

In a 100 mL round-bottomed flask dimedone (1 mmol), ethyl acetoacetate (1 mmol), ammonium acetate (1 mml) and different aryl aldehyde derivative (1 mmol) were added. Copper nitrate trihydrate ($\text{Cu}(\text{NO}_3)_2 \cdot 3\text{H}_2\text{O}$ (10 mol%) was added as catalyst in this flask and heated at 80-90 °C with vigorous mixing. Thin layer chromatography (TLC) was used to predict reaction progress. As the reaction was completed, the solid product was washed with distilled water then hexane after that with hot hexane to get pure product. Ethanol was used for crystallization of obtained product to get pure product. Compounds **4**, **8**, **17**, **19**, **20**, **24**, and **27** found to be new while remaining compounds are already reported in literature [19-26]. Various spectroscopic techniques were used to characterize the synthetic compounds. A complete spectral data of all compounds is as follows.

Ethyl-2,7,7-trimethyl-5-oxo-4-phenyl-1,4,5,6,7,8-hexahydroquinoline-3-carboxylate (1) [27]

State: solid; Color: light green; Yield: 65%; M.P.: 156-159 °C; R_f : 0.48 (dichloromethane/methanol, 9.6:0.4); $^1\text{H-NMR}$ (300 MHz, $\text{DMSO-}d_6$): δ_H 9.04 (s, 1H, NH), 7.19 (m, 5H, H-2', H-3', H-4', H-5', H-6'), 4.83 (s, 1H, H-4), 3.99 (q, $J_{\text{CH}_2, \text{CH}_3} = 6.9 \text{ Hz}$, 2H, CH_2), 2.43 (d, $J_{\text{H}_a, \text{H}_b} = 17.1 \text{ Hz}$, 1H, H_a), 2.29 (ovp, 1H, H_b), 2.26 (s, 3H, CH_3), 2.17 (d, $J_{\text{H}_a', \text{H}_b'} = 16.2 \text{ Hz}$, 1H, H_a'), 1.98 (d, $J_{\text{H}_b', \text{H}_a'} = 15.9 \text{ Hz}$, 1H, H_b'), 1.13 (t, $J_{\text{CH}_3, \text{CH}_2} = 7.2 \text{ Hz}$, 3H, CH_3),

0.99 (s, 3H, CH₃), 0.82 (s, 3H, CH₃); EI-MS *m/z* (% rel. abund.): 339 (M⁺, 34), 310 (19), 294 (14), 262 (100), 234 (59), 178 (10), 150 (5), 115 (2), 105 (3) 77 (1).

Ethyl-4-(3,4-dimethoxyphenyl)-2,7,7-trimethyl-5-oxo-1,4,5,6,7,8-hexahydroquinoline-3-carboxylate (2) [28]

State: solid; Color: white; Yield: 65%, M.P.: 198-200 °C; R_f: 0.43 (dichloromethane/methanol, 9.6:0.4); ¹H-NMR (300 MHz, DMSO-*d*₆): δ_H 9.00 (s, 1H, NH), 6.76 (ovp, 2H, H-2', H-5'), 6.62 (dd, *J*_{6',2'} = 1.8 Hz, *J*_{6',5'} = 6.6 Hz, 1H, H-6'), 4.77 (s, 1H, H-4), 4.02 (q, *J*_{CH₂,CH₃} = 6.9 Hz, 2H, CH₂), 3.65 (s, 3H, OCH₃), 3.64 (s, 3H, OCH₃), 2.44 (d, *J*_{H_a,H_b} = 17.1 Hz, 1H, H_a), 2.29 (ovp, 1H, H_b), 2.25 (s, 3H, CH₃), 2.19 (d, *J*_{H_a',H_b'} = 16.2 Hz, 1H, H_a'), 2.00 (d, *J*_{H_b',H_a'} = 16.2 Hz, 1H, H_b'), 1.17 (t, *J*_{CH₃,CH₂} = 7.2 Hz, 3H, CH₃), 1.00 (s, 3H, CH₃), 0.87 (s, 3H, CH₃); EI-MS *m/z* (% rel. abund.): 399 (M⁺, 93), 370 (27), 354 (12), 326 (22), 262 (100), 252 (25), 234 (35), 178 (10), 83 (3).

Ethyl-4-(3,5-dimethoxyphenyl)-2,7,7-trimethyl-5-oxo-1,4,5,6,7,8-hexahydroquinoline-3-carboxylate (3) [27]

State: Solid; Color: white; Yield: 70%, M.P.: 152-155 °C; R_f: 0.42 (dichloromethane/methanol, 9.6:0.4); ¹H-NMR (400 MHz, DMSO-*d*₆): δ_H 9.03 (s, 1H, NH), 6.27 (d, *J*_{2',4'/6',4'} = 2.0 Hz, 2H, H-2', H-6'), 6.23 (d, *J*_{4',2'/4',6'} = 2.4 Hz, 1H, H-4'), (m, 1H, H-4'), 4.79 (s, 1H, H-4), 4.02 (q, *J*_{CH₂,CH₃} = 7.2 Hz, 2H, CH₂), 3.64 (s, 6H, (OCH₃)₂), 2.42 (d, *J*_{H_a,H_b} = 17.2 Hz, 1H, H_a), 2.30 (ovp, 1H, H_b), 2.25 (s, 3H, CH₃), 2.18 (d, *J*_{H_a',H_b'} = 16.0 Hz, 1H, H_a'), 2.01 (d, *J*_{H_b',H_a'} = 16.0 Hz, 1H, H_b'), 1.16 (t, *J*_{CH₃,CH₂} = 6.8 Hz, 3H, CH₃), 1.00 (s, 3H, CH₃), 0.88 (s, 3H, CH₃); EI-MS *m/z* (% rel. abund.): 399 (M⁺, 83), 384 (3), 370 (13), 354 (16), 326 (26), 296 (5), 262 (100), 246 (5), 234 (83), 178 (14), 150 (5), 138 (8), 77 (2).

Ethyl-4-(2,6-dimethoxyphenyl)-2,7,7-trimethyl-5-oxo-1,4,5,6,7,8-hexahydroquinoline-3-carboxylate (4)

State: Solid; Color: White; Yield: 65%, M.P.: 220-223 °C; R_f: 0.45 (dichloromethane/methanol, 9.6:0.4); ¹H-NMR (400 MHz, DMSO-*d*₆): δ_H 8.77 (s, 1H, NH), 6.99 (t, *J*_{4',3'/4',5'} = 8.4 Hz, 1H, H-4'), 6.48 (d, *J*_{3',4'/5',4'} = 8.4 Hz, 2H, H-2', H-5'), 5.44 (s, 1H, H-4), 3.85 (q, *J*_{CH₂,CH₃} = 7.2 Hz, 2H, CH₂), 3.68 (s, 6H, (OCH₃)₂), 2.33 (d, *J*_{H_a,H_b} = 16.4 Hz, 1H, H_a'), 2.15 (ovp, 1H, H_b'), 2.14 (s, 3H, CH₃), 2.06 (d, *J*_{H_a',H_b'} = 16.0 Hz, 1H, H_a'), 1.82 (d, *J*_{H_b',H_a'} = 16.0 Hz, 1H, H_b'), 1.04 (t, *J*_{CH₃,CH₂} = 7.2 Hz, 3H, CH₃), 0.96 (s, 3H, CH₃), 0.78 (s, 3H, CH₃); ¹³C-NMR (75 MHz, DMSO-

d_6): δ 193.4, 150.9, 150.1, 144.8, 142.9, 126.6, 123.0 108.0, 103.9, 101.2, 58.3, 55.4, 50.6, 39.7, 31.7, 29.3 26.6, 25.9, 18.1, 13.9; EI-MS m/z (% rel. abund.): 399 (M^+ , 100), 384 (11), 370 (86), 354 (14), 322 (16), 262 (56), 257 (29), 241 (34), 234 (20), 189 (14), 115 (3), 83 (5); HREI-MS Calcd for $C_{23}H_{29}O_5N_1$: $m/z = 399.20424$, Found 399.2046.

Ethyl-4-(2,5-dimethoxyphenyl)-2,7,7-trimethyl-5-oxo-1,4,5,6,7,8-hexahydroquinoline-3-carboxylate (5) [29]

State: Solid; Color: White; Yield: 62%, M.P.: 169-172 °C; R_f : 0.44 (dichloromethane/methanol, 9.6:0.4); 1H -NMR (300 MHz, DMSO- d_6): δ_H 8.93 (s, 1H, NH), 6.75 (d, $J_{3',4'} = 8.4$ Hz, 1H, H-3'), 6.62 (ovp, 2H, H-4', H-6'), 4.97 (s, 1H, H-4), 3.92 (q, $J_{CH_2,CH_3} = 2.1$ Hz, 2H, CH₂), 3.63 (s, 3H, OCH₃), 3.61 (s, 3H, OCH₃), 2.41 (d, $J_{H_a,H_b} = 16.8$ Hz, 1H, H_a), 2.25 (d, $J_{H_b,H_a} = 18.0$ Hz, 1H, H_b), 2.16 (s, 3H, CH₃), 2.13 (d, $J_{H_a',H_b'} = 16.2$ Hz, 1H, H_{a'}), 1.91 (d, $J_{H_b',H_a'} = 15.9$ Hz, 1H, H_{b'}), 1.12 (t, $J_{CH_3,CH_2} = 6.9$ Hz, 3H, CH₃), 0.98 (s, 3H, CH₃), 0.84 (s, 3H, CH₃); EI-MS m/z (% rel. abund.): 399 (M^+ , 55), 366 (46), 354 (6), 322 (7), 262 (76), 257 (100), 234 (16), 200 (18), 189 (3), 138 (5), 83 (11), 55 (4).

Ethyl-2,7,7-trimethyl-5-oxo-4-(3,4,5-trimethoxyphenyl)-1,4,5,6,7,8-hexahydroquinoline-3-carboxylate (6) [30]

State: Solid; Color: White; Yield: 65%, M.P.: 178-180 °C; R_f : 0.43 (dichloromethane/methanol, 9.6:0.4); 1H -NMR (300 MHz, DMSO- d_6): δ_H 9.06 (s, 1H, NH), 6.39 (s, 2H, H-5', H-6'), 4.80 (s, 1H, H-4), 4.06 (q, $J_{CH_2,CH_3} = 6.9$ Hz, 2H, CH₂), 3.65 (s, 6H, (OCH₃)₂), 3.57 (s, 3H, OCH₃), 2.41 (ovp, 1H, H_a), 2.33 (d, $J_{H_b,H_a} = 17.4$ Hz, 1H, H_b), 2.25 (s, 3H, CH₃), 2.21 (d, $J_{H_a',H_b'} = 16.2$ Hz, 1H, H_{a'}), 2.03 (d, $J_{H_b',H_a'} = 16.2$ Hz, 1H, H_{b'}), 1.20 (t, $J_{CH_3,CH_2} = 7.2$ Hz, 3H, CH₃), 1.01 (s, 3H, CH₃), 0.92 (s, 3H, CH₃); EI-MS m/z (% rel. abund.): 429 (M^+ , 76), 400 (14), 384 (10), 356 (12), 262 (100), 234 (29), 189 (2), 168 (9), 150 (3).

Ethyl-2,7,7-trimethyl-5-oxo-4-(2,3,4-trimethoxyphenyl)-1,4,5,6,7,8-hexahydroquinoline-3-carboxylate (7)

State: Solid; Color: White; Yield: 65%, M.P.: 159-162 °C; R_f : 0.43 (dichloromethane/methanol, 9.6:0.4); 1H -NMR (400 MHz, DMSO- d_6): δ_H 9.89 (s, 1H, NH), 6.78 (d, $J_{6',5'} = 8.8$ Hz, 1H, H-6'), 6.59 (d, $J_{5',6'} = 8.8$ Hz, 1H, H-5'), 4.95 (s, 1H, H-4), 3.92 (q, $J_{CH_2,CH_3} = 2.4$ Hz, 2H, CH₂), 3.76 (s, 3H, OCH₃), 3.69 (s, 3H, OCH₃), 3.63 (s, 3H, OCH₃), 2.38 (d, $J_{H_a,H_b} = 17.2$ Hz, 1H, H_a), 2.25 (d, $J_{H_b,H_a} = 17.2$ Hz, 1H, H_b), 2.17 (s, 3H, CH₃), 2.12 (d, $J_{H_a',H_b'} = 16.0$ Hz, 1H, H_{a'}), 1.93

(d, $J_{Hb',Ha'} = 16.0$ Hz, 1H, H_{b'}), 1.13 (t, $J_{CH_3,CH_2} = 7.2$ Hz, 3H, CH₃), 0.98 (s, 3H, CH₃), 0.87 (s, 3H, CH₃); EI-MS m/z (% rel. abund.): 429 (M⁺, 30), 409 (100), 398 (59), 384 (4), 352 (9), 325 (3), 273 (8), 262 (35), 234 (12), 189 (3), 161 (2), 83 (4).

Ethyl-4-(3-ethoxy-4-methoxyphenyl)-2,7,7-trimethyl-5-oxo-1,4,5,6,7,8-hexahydroquinoline-3-carboxylate (8)

State: Solid; Color: White; Yield: 60%, M.P.: 173-176 °C; R_f: 0.40 (dichloromethane/methanol, 9.6:0.4); ¹H-NMR (300 MHz, DMSO-*d*₆): δ_H 8.99 (s, 1H, NH), 6.75 (ovp, 2H, H-2', H-5'), 6.61 (d, $J_{6',5'} = 8.1$ Hz, 1H, H-6'), 4.76 (s, 1H, H-4), 4.01 (q, $J_{CH_2,CH_3} = 6.9$ Hz, 2H, CH₂), 3.89 (q, $J_{CH_2,CH_3'} = 5.1$ Hz, 2H, CH₂'), 3.65 (s, 3H, OCH₃) 2.43 (d, $J_{Ha,Hb} = 17.4$ Hz, 1H, H_a), 2.28 (ovp, 1H, H_b), 2.25 (s, 3H, CH₃), 2.18 (d, $J_{Ha',Hb'} = 15.9$ Hz, 1H, 8-Ha), 1.99 (d, $J_{Hb',Ha'} = 16.2$ Hz, 1H, H_{b'}), 1.29 (t, $J_{CH_3',CH_2'} = 6.9$ Hz, 3H, CH₃'), 1.16 (t, $J_{CH_3,CH_2} = 6.9$ Hz, 3H, CH₃), 0.99 (s, 3H, CH₃), 0.85 (s, 3H, CH₃); ¹³C-NMR (75 MHz, DMSO-*d*₆): δ_c 194.2, 166.9, 149.2, 147.1, 147.0, 144.5, 140.3, 119.2, 113.0, 111.5, 110.0, 103.7, 63.5, 58.9, 55.3, 50.2, 39.5, 35.0, 32.0, 29.1, 26.3, 18.1, 14.7, 14.1; EI-MS m/z (% rel. abund.): 413 (M⁺, 89), 384 (26), 368 (13), 340 (17), 302 (19), 273 (7), 262 (100), 234 (25), 218 (2), 189 (3), 178 (8), 152 (8), 83 (8), 54 (3); HREI-MS Calcd for C₂₄H₃₁O₅N₁: $m/z = 413.2225$, Found 413.2202.

Ethyl-4-(2-fluorophenyl)-2,7,7-trimethyl-5-oxo-1,4,5,6,7,8-hexahydroquinoline-3-carboxylate (9)

State: Solid; Color: Light green; Yield: 59%, M.P.: 160-162 °C; R_f: 0.37 (dichloromethane/methanol, 9.6:0.4); ¹H-NMR (400 MHz, DMSO-*d*₆): δ_H 9.04 (s, 1H, NH), 7.20 (t, $J_{4',3'/4',5'} = 7.2$ Hz, 1H, H-4'), 7.09 (m, 1H, H-3') 7.02 (overlap multiplet, 2H, H-5', H-6'), 5.03 (s, 1H, H-4), 3.93 (q, $J_{CH_2,CH_3} = 7.2$ Hz, 2H, CH₂), 2.42 (d, $J_{Ha,Hb} = 17.2$ Hz, 1H, H_a), 2.27 (ovp, 1H, 6-H_b), 2.23 (s, 3H, CH₃), 2.15 (d, $J_{Ha',Hb'} = 15.6$ Hz, 1H, H_{a'}), 1.92 (d, $J_{Hb',Ha} = 16.4$ Hz, 1H, H_{b'}), 1.09 (t, $J_{CH_3,CH_2} = 7.2$ Hz, 3H, CH₃), 0.99 (s, 3H, CH₃), 0.82 (s, 3H, CH₃); EI-MS m/z (% rel. abund.): 357 (M⁺, 26), 336 (4), 328 (16), 312 (7), 284 (9), 262 (100), 234 (30), 198 (3), 178 (4), 157 (3), 133 (1).

Ethyl-4-(2-fluoro-4-methoxyphenyl)-2,7,7-trimethyl-5-oxo-1,4,5,6,7,8-hexahydroquinoline-3-carboxylate (10)

State: Solid; Color: Green; Yield: 52%, M.P.: 180-182 °C; R_f: 0.32 (dichloromethane/methanol, 9.6:0.4); ¹H-NMR (400 MHz, DMSO-*d*₆): δ_H 9.00 (s, 1H, NH), 7.07 (t, $J_{H-3',F} = 8.4$ Hz, 1H, H-

3'), 6.60 (overlap multiplet 2H, H-5', H-6'), 4.94 (s, 1H, H-4), 3.94 (q, $J_{CH_2,CH_3} = 7.2$ Hz, 2H, CH₂), 3.67 (s, 3H, OCH₃), 2.41 (d, $J_{H_a,H_b} = 16.8$ Hz, 1H, H_a), 2.25 (ovp, 1H, H_b), 2.22 (s, 3H, CH₃), 2.14 (d, $J_{H_a',H_b'} = 16.0$ Hz, 1H, H_{a'}), 1.92 (d, $J_{H_b',H_a'} = 16.0$ Hz, 1H, H_{b'}), 1.11 (t, $J_{CH_3,CH_2} = 7.2$ Hz, 3H, CH₃), 0.99 (s, 3H, CH₃), 0.83 (s, 3H, CH₃); EI-MS m/z (% rel. abund.): 387 (M⁺, 37), 358 (14), 342 (9), 314 (17), 262 (100), 234 (15), 189 (4), 178 (4), 150 (1), 126 (2), 83 (1).

Ethyl-4-(4-fluoro-3-methoxyphenyl)-2,7,7-trimethyl-5-oxo-1,4,5,6,7,8-hexahydroquinoline-3-carboxylate (11)

State: Solid; Color: Green; Yield: 52%, M.P.: 212-215 °C; R_f: 0.32 (dichloromethane/methanol, 9.6:0.4); ¹H-NMR (400 MHz, DMSO-*d*₆): δ_H 9.06 (s, 1H, NH), 7.02 (m, 1H, H-5'), 6.89 (dd, $J_{6',2'} = 1.6$ Hz, $J_{6',5'} = 6.8$ Hz, 1H, H-6'), 6.66 (m, 1H, H-2'), 4.82 (s, 1H, H-4), 4.01 (q, $J_{CH_2,CH_3} = 6.8$ Hz, 2H, CH₂), 3.73 (s, 3H, OCH₃), 2.43 (d, $J_{H_a,H_b} = 17.2$ Hz, 1H, H_a), 2.30 (ovp, 1H, H_b), 2.27 (s, 3H, CH₃), 2.18 (d, $J_{H_a',H_b'} = 16.0$ Hz, 1H, H_{a'}), 2.00 (d, $J_{H_b',H_a'} = 16.0$ Hz, 1H, H_{b'}), 1.15 (t, $J_{CH_3,CH_2} = 7.2$ Hz, 3H, CH₃), 1.00 (s, 3H, CH₃), 0.85 (s, 3H, CH₃); EI-MS m/z (% rel. abund.): 387 (M⁺, 22), 358 (7), 342 (3), 314 (5), 262 (100), 234 (15), 178 (3), 150 (1), 77 (1).

Ethyl-4-(4-chlorophenyl)-2,7,7-trimethyl-5-oxo-1,4,5,6,7,8-hexahydroquinoline-3-carboxylate (12) [31]

State: Solid; Color: White; Yield: 67%, M.P.: 224-226 °C; R_f: 0.40 (dichloromethane/methanol, 9.6:0.4); ¹H-NMR (400 MHz, DMSO-*d*₆): δ_H 9.08 (s, 1H, NH), 7.24 (d, $J_{3',2'/5',6'} = 8.4$ Hz, 2H, H-3', H-5'), 7.14 (d, $J_{2',3'/6',5'} = 8.4$ Hz, 2H, H-2', H-6'), 4.82 (s, 1H, H-4), 3.98 (q, $J_{CH_2,CH_3} = 7.2$ Hz, 2H, CH₂), 2.42 (d, $J_{H_a,H_b} = 17.2$ Hz, 1H, H_a), 2.27 (s, 3H, CH₃), 2.24 (ovp, 1H, H_b), 2.17 (d, $J_{H_a',H_b'} = 16.4$ Hz, 1H, H_{a'}), 1.98 (d, $J_{H_b',H_a'} = 16.4$ Hz, 1H, H_{b'}), 1.12 (t, $J_{CH_3,CH_2} = 6.8$ Hz, 3H, CH₃), 0.99 (s, 3H, CH₃), 0.81 (s, 3H, CH₃); EI-MS m/z (% rel. abund.): 373 (M⁺, 90.3), 344 (29), 328 (24), 262 (100), 252 (15), 234 (68), 178 (10), 150 (6), 105 (2), 83 (2).

Ethyl-4-(2-chlorophenyl)-2,7,7-trimethyl-5-oxo-1,4,5,6,7,8-hexahydroquinoline-3-carboxylate (13) [32]

State: Solid; Color: White; Yield: 60%, M.P.: 169-172 °C; R_f: 0.41 (dichloromethane/methanol, 9.6:0.4); ¹H-NMR (400 MHz, DMSO-*d*₆): δ_H 9.05 (s, 1H, NH), 7.27 (d, $J_{3',4'} = 7.2$ Hz, 1H, H-3'), 7.21 (ovp, 2H, H-4', H-6'), 7.07 (t, $J_{5',4'/5',6'} = 7.6$ Hz, 1H, H-5'), 5.16 (s, 1H, H-4), 3.93 (q, $J_{CH_2,CH_3} = 4.4$ Hz, 2H, CH₂), 2.42 (d, $J_{H_a,H_b} = 16.8$ Hz, 1H, H_a), 2.26 (ovp, 1H, H_b), 2.22 (s, 3H, CH₃), 2.14 (d, $J_{H_a',H_b'} = 16.4$ Hz, 1H, H_{a'}), 1.91 (d, $J_{H_b',H_a'} = 16.0$ Hz, 1H, H_{b'}), 1.08 (t, J_{CH_3,CH_2}

= 7.2 Hz, 3H, CH₃), 0.99 (s, 3H, CH₃), 0.82 (s, 3H, CH₃); EI-MS *m/z* (% rel. abund.): 373 (M⁺, 31), 338 (53), 328 (12), 262 (100), 252 (4), 234 (51), 227 (14), 178 (10), 150 (5), 115 (1), 83(2), 55(1).

Ethyl-4-(2-chloro-3-methoxyphenyl)-2,7,7-trimethyl-5-oxo-1,4,5,6,7,8-hexahydroquinoline-3-carboxylate (14) [31]

State: Solid; Color: Green; Yield: 56%, M.P.: 181-184 °C; R_f: 0.38 (dichloromethane/methanol, 9.6:0.4); ¹H-NMR (400 MHz, DMSO-*d*₆): δ_H 9.02 (s, 1H, NH), 7.12 (t, *J*_{5',4'/5',6'} = 8.0 Hz, 1H, H-5'), 6.86 (d, *J*_{4',5'} = 7.6 Hz, 1H, H-4'), 6.81 (d, *J*_{6',5'} = 8.0 Hz, 1H, H-6'), 5.22 (s, 1H, H-4), 3.92 (q, *J*_{CH₂,CH₃} = 7.2 Hz, 2H, CH₂), 3.76 (s, 3H, OCH₃), 2.42 (d, *J*_{Ha,Hb} = 16.8 Hz, 1H, 6-H_a), 2.25 (ovp, 1H, H_b), 2.21 (s, 3H, CH₃), 2.13 (d, *J*_{Ha',Hb'} = 16.4 Hz, 1H, H_{a'}), 1.90 (d, *J*_{Hb',Ha'} = 16.0 Hz, 1H, H_{b'}), 1.08 (t, *J*_{CH₃,CH₂} = 6.8 Hz, 3H, CH₃), 0.98 (s, 3H, CH₃), 0.82 (s, 3H, CH₃); EI-MS *m/z* (% rel. abund.): 403 (M⁺, 10), 368 (60), 294 (3), 262 (100), 234 (32), 201 (7), 178 (5), 150 (2), 115 (1), 83(3).

Ethyl-4-(4-bromophenyl)-2,7,7-trimethyl-5-oxo-1,4,5,6,7,8-hexahydroquinoline-3-carboxylate (15) [33]

State: Solid; Color: White; Yield: 52%, M.P.: 175-177 °C; R_f: 0.40 (dichloromethane/methanol, 9.6:0.4); ¹H-NMR (400 MHz, DMSO-*d*₆): δ_H 9.08 (s, 1H, NH), 7.37 (d, *J*_{3',2'/5',6'} = 8.4 Hz, 2H, H-3', H-5'), 7.09 (d, *J*_{2',3'/6',5'} = 8.0 Hz, 2H, H-2', H-6'), 4.80 (s, 1H, H-4), 3.98 (q, *J*_{CH₂,CH₃} = 7.2 Hz, 2H, CH₂), 2.42 (d, *J*_{Ha,Hb} = 17.2 Hz, 1H, H_a), 2.27 (s, 3H, CH₃), 2.24 (ovp, 1H, H_b), 2.17 (d, *J*_{Ha',Hb'} = 16.0 Hz, 1H, H_{a'}), 1.97 (d, *J*_{Hb',Ha'} = 15.6 Hz, 1H, H_{b'}), 1.12 (t, *J*_{CH₃,CH₂} = 6.8 Hz, 3H, CH₃), 0.99 (s, 3H, CH₃), 0.81 (s, 3H, CH₃); EI-MS *m/z* (% rel. abund.): 417 (M⁺, 63), 419 (M+2, 57.5), 387 (18), 371 (13), 345 (13), 262 (100), 234 (60), 189 (4), 178 (10), 150 (5), 105 (2), 77 (2).

Ethyl-4-(4-bromo-2-fluorophenyl)-2,7,7-trimethyl-5-oxo-1,4,5,6,7,8-hexahydroquinoline-3-carboxylate (16) [34]

State: Solid; Color: Green; Yield: 60%, M.P.: 180-182 °C; R_f: 0.39 (dichloromethane/methanol, 9.6:0.4); ¹H-NMR (400 MHz, DMSO-*d*₆): δ_H 9.10 (s, 1H, NH), 7.28 (overlap multiplet, 2H, H-5' H-6'), 7.14 (t, *J*_{3',F} = 8.4 Hz, 1H, H-3'), 4.99 (s, 1H, H-4), 3.94 (q, *J*_{CH₂,CH₃} = 7.2 Hz, 2H, CH₂), 2.42 (d, *J*_{Ha,Hb} = 16.8 Hz, 1H, H_a), 2.26 (ovp, 1H, H_b), 2.24 (s, 3H, CH₃), 2.15 (d, *J*_{Ha',Hb'} = 16.4 Hz, 1H, H_{a'}), 1.93 (d, *J*_{Hb',Ha'} = 16.0 Hz, 1H, H_{b'}), 1.09 (t, *J*_{CH₃,CH₂} = 7.2 Hz, 3H, CH₃),

0.99 (s, 3H, CH₃), 0.82 (s, 3H, CH₃); EI-MS *m/z* (% rel. abund.): 435 (M⁺, 22), 437 (M⁺+2, 20.6), 408 (8), 390 (5), 362 (6), 262 (100), 234 (19), 178 (3), 150 (1).

Ethyl-4-(5-bromo-2-fluorophenyl)-2,7,7-trimethyl-5-oxo-1,4,5,6,7,8-hexahydroquinoline-3-carboxylate (17)

State: Solid; Color: White; Yield: 60%, M.P.: 208-210 °C; R_f: 0.41 (dichloromethane/methanol, 9.6:0.4); ¹H-NMR (400 MHz, DMSO-*d*₆): δ_H 9.13 (s, 1H, NH), 7.30(ovp, 2H, H-4', H-6'), 7.00 (t, *J*_{3',F/3',4'} = 9.6 Hz, 1H, H-3'), 4.96 (s, 1H, H-4), 3.96 (q, *J*_{CH₂,CH₃} = 7.2 Hz, 2H, CH₂), 2.43 (d, *J*_{Ha,Hb} = 17.2 Hz, 1H, H_a), 2.28 (ovp, 1H, H_b), 2.24 (s, 3H, CH₃), 2.16 (d, *J*_{Ha',Hb'} = 16.4 Hz, 1H, H_{a'}), 1.95 (d, *J*_{Hb',Ha'} = 16.4 Hz, 1H, H_{b'}), 1.10 (t, *J*_{CH₃,CH₂} = 7.2Hz, 3H, CH₃), 0.99 (s, 3H, CH₃), 0.84 (s, 3H, CH₃); ¹³C-NMR (75 MHz, DMSO-*d*₆): δ 193.9, 166.3, 150.0, 145.8, 136.8, 133.3, 130.3, 130.2, 117.5, 117.2, 108.2, 101.7, 59.0, 50.0, 39.3, 32.0, 32.0, 29.0, 26.0, 18.1, 13.8; EI-MS *m/z* (% rel. abund.): 435 (M⁺, 51), 437 (M+2, 57.0), 406 (28), 392 (14), 362 (15), 262 (100), 234 (63), 199 (4), 178 (9), 150 (3), 94 (2); HREI-MS Calcd for C₂₁H₂₃O₄NBrF: *m/z* = 435.0860, Found 435.0845.94 (3), 262 (100), 234 (32), 201 (7), 178 (5), 150 (2), 115 (1), 83(3).

Ethyl-4-(2-bromo-4,5-dimethoxyphenyl)-2,7,7-trimethyl-5-oxo-1,4,5,6,7,8-hexahydroquinoline-3-carboxylate (18)

State: Solid; Color: Green; Yield: 62%, M.P.: 168-170 °C; R_f: 0.42 (dichloromethane/methanol, 9.6:0.4); ¹H-NMR (300 MHz, DMSO-*d*₆): δ_H 9.04 (s, 1H, NH), 6.87 (s, 1H, H-3'), 6.76 (s, 1H, H-6'), 5.03 (s, 1H, H-4), 3.98 (q, *J*_{CH₂,CH₃} = 7.2 Hz, 2H, CH₂), 3.69 (s, 3H, OCH₃), 3.61 (s, 3H, OCH₃), 2.44 (d, *J*_{Ha,Hb} = 17.1Hz, 1H, H_a), 2.26 (ovp, 1H, H_b), 2.22 (s, 3H, CH₃), 2.16 (d, *J*_{Ha',Hb'} = 15.9 Hz, 1H, H_{a'}), 1.93 (d, *J*_{Hb',Ha'} = 16.2 Hz, 1H, H_{b'}), 1.13 (t, *J*_{CH₃,CH₂} = 7.2 Hz, 3H, CH₃), 0.99 (s, 3H, CH₃), 0.84 (s, 3H, CH₃); EI-MS *m/z* (% rel. abund.): 478 (M⁺, 2), 448 (3), 434 (12), 408 (28), 398 (100), 370 (31), 352 (23), 324 (27), 308 (12), 272 (13), 262 (79), 234 (65), 218 (19), 178 (23), 150 (10), 105(4), 83(5).

Ethyl-4-(4-bromo-3,5-dimethoxyphenyl)-2,7,7-trimethyl-5-oxo-1,4,5,6,7,8-hexahydroquinoline-3-carboxylate (19)

State: Solid; Color: White; Yield: 63%, M.P.: 223-225 °C; R_f: 0.42 (dichloromethane/methanol, 9.6:0.4); ¹H-NMR (300 MHz, DMSO-*d*₆): δ_H 9.12 (s, 1H, NH), 6.46 (s, 2H, H-2', H-6'), 4.85 (s, 1H, H-4), 4.05 (q, *J*_{CH₂,CH₃} = 7.2 Hz, 2H, CH₂), 3.71 (s, 6H, (OCH₃)₂), 2.42 (ovp, 1H, H_a),

2.33 (ovp, 1H, H_b), 2.27 (s, 3H, CH₃), 2.22 (d, $J_{H_a',H_b'} = 16.2$ Hz, 1H, H_{a'}), 2.03 (d, $J_{H_b',H_a'} = 16.2$ Hz, 1H_{b'}), 1.18 (t, $J_{CH_3,CH_2} = 6.9$ Hz, 3H, CH₃), 1.01 (s, 3H, CH₃), 0.89 (s, 3H, CH₃); ¹³C-NMR (75 MHz, DMSO-*d*₆): δ_c 194.3, 166.7, 155.9, 149.9, 148.8, 145.2, 109.3, 104.0, 103.1, 97.1, 59.1, 55.9, 50.1, 39.5, 36.1, 32.0, 29.1, 26.2, 18.2, 14.2; EI-MS *m/z* (% rel. abund.): 477 (M⁺, 63), 479 (M+2, 58.7), 450 (11), 432 (10), 406 (10), 366 (33), 337 (53), 262 (100), 234 (50), 189 (3), 178 (11), 115 (4), 83 (17), 55 (6). HREI-MS Calcd for C₂₃H₂₈O₅N₁Br: *m/z* = 477.1170, Found 477.1151.

Ethyl-4-(2-bromo-6-methoxyphenyl)-2,7,7-trimethyl-5-oxo-1,4,5,6,7,8-hexahydroquinoline-3-carboxylate (20)

State: Solid; Color: Green; Yield: 66%, M.P.: 194-197 °C; R_f: 0.37 (dichloromethane/methanol, 9.6:0.4); ¹H-NMR (300 MHz, DMSO-*d*₆): δ_H 9.01 (s, 1H, NH), 7.22 (ovp, 2H, H-4', H-5'), 6.83 (d, $J_{3',4'} = 8.4$ Hz, 1H, H-3') 4.92 (s, 1H, H-4), 3.92 (q, $J_{CH_2,CH_3} = 2.7$ Hz, 2H, CH₂), 3.67 (s, 3H, OCH₃), 2.42 (d, $J_{H_a,H_b} = 17.1$ Hz, 1H, H_a), 2.24 (ovp, 1H, H_b), 2.18 (s, 3H, CH₃), 2.14 (d, $J_{H_a',H_b'} = 16.2$ Hz, 1H, H_{a'}), 1.91 (d, $J_{H_b',H_a'} = 15.9$ Hz, 1H, H_{b'}), 1.12 (t, $J_{CH_3,CH_2} = 7.2$ Hz, 3H, CH₃), 0.99 (s, 3H, CH₃), 0.82 (s, 3H, CH₃); ¹³C-NMR (75 MHz, DMSO-*d*₆): δ_c 193.8, 166.9, 156.7, 150.3, 145.0, 136.8, 133.1, 129.3, 113.4, 111.0, 107.8, 101.7, 58.8, 55.4, 50.2, 39.5, 33.9, 31.9, 29.2, 25.9, 18.0, 13.9; EI-MS *m/z* (% rel. abund.): 447 (M⁺, 60.6), 449 (M+2, 57.8), 417 (48), 403 (9), 374 (8), 288 (6), 262 (100), 234 (43), 190 (8), 178 (14), 150 (6), 105 (2), 83 (2). HREI-MS Calcd for C₂₂H₂₆O₄N₁Br: *m/z* = 447.1040, Found 447.1045.

Ethyl-4-(4-hydroxyphenyl)-2,7,7-trimethyl-5-oxo-1,4,5,6,7,8-hexahydroquinoline-3-carboxylate (21) [34]

State: Solid; Color: Off white; Yield: 60%, M.P.: 224-226 °C; R_f: 0.30 (dichloromethane/methanol, 9.6:0.4); ¹H-NMR (400 MHz, DMSO-*d*₆): δ_H 8.99 (s, 1H, OH), 8.93 (s, 1H, NH), 6.92 (d, $J_{3',2'/5',6'} = 8.4$ Hz, 2H, H-3', H-5'), 6.54 (d, $J_{2',3'/6',5'} = 8.4$ Hz, 2H, H-2', H-6'), 4.72 (s, 1H, H-4), 3.98 (q, $J_{CH_2,CH_3} = 6.8$ Hz, 2H, CH₂), 2.40 (d, $J_{H_a,H_b} = 17.2$ Hz, 1H, H_a), 2.27 (ovp, 1H, H_b), 2.24 (s, 3H, CH₃), 2.15 (d, $J_{H_a',H_b'} = 16.0$ Hz, 1H, H_{a'}), 1.97 (d, $J_{H_b',H_a'} = 15.6$ Hz, 1H, H_{b'}), 1.14 (t, $J_{CH_3,CH_2} = 7.2$ Hz, 3H, CH₃), 0.99 (s, 3H, CH₃), 0.84 (s, 3H, CH₃); EI-MS *m/z* (% rel. abund.): 355 (M⁺, 92), 340 (5), 326 (30), 310 (16), 282 (27), 262 (100), 252 (3), 234 (39), 189 (4), 178 (7), 150 (3), 83 (1), 65 (1).

Ethyl-4-(3-hydroxyphenyl)-2,7,7-trimethyl-5-oxo-1,4,5,6,7,8-hexahydroquinoline-3-carboxylate (22) [33]

State: Solid; Color: Off white; Yield: 60%, M.P.: 192-195 °C; R_f : 0.31 (dichloromethane/methanol, 9.6:0.4); $^1\text{H-NMR}$ (400 MHz, DMSO- d_6): δ_H 9.04 (s, 1H, OH), 8.99 (s, 1H, NH), 6.94 (t, $J_{5',4'/5',6'} = 7.6$ Hz, 1H, H-5'), 6.57 (ovp, 2H, H-2', H-4'), 6.44 (d,d, $J_{6',2'} = 2.0$ Hz, $J_{6',5'} = 6.8$ Hz, 1H, H-6'), 4.77 (s, 1H, H-4), 3.99 (q, $J_{\text{CH}_2,\text{CH}_3} = 7.2$ Hz, 2H, CH₂), 2.41 (d, $J_{\text{H}_a,\text{H}_b} = 16.8$ Hz, 1H, H_a), 2.28 (overlapping multiplet, 1H, H_b), 2.25 (s, 3H, CH₃), 2.16 (d, $J_{\text{H}_a',\text{H}_b'} = 16.0$ Hz, 1H, H_{a'}), 1.99 (d, $J_{\text{H}_b',\text{H}_a'} = 16.0$ Hz, 1H, H_{b'}), 1.15 (t, $J_{\text{CH}_3,\text{CH}_2} = 7.2$ Hz, 3H, CH₃), 0.99 (s, 3H, CH₃), 0.85 (s, 3H, CH₃); EI-MS m/z (% rel. abund.): 355 (M⁺, 51), 326 (23), 310 (18), 282 (15), 262 (100), 252 (12), 234 (59), 178 (10), 150 (6), 105 (2), 77 (2), 63 (1).

Ethyl-4-(3-hydroxy-4-methoxyphenyl)-2,7,7-trimethyl-5-oxo-1,4,5,6,7,8-hexahydroquinoline-3-carboxylate (23) [33]

State: Solid; Color: Off white; Yield: 52%, M.P.: 209-211 °C; R_f : 0.33 (dichloromethane/methanol, 9.6:0.4); $^1\text{H-NMR}$ (400 MHz, DMSO- d_6): δ_H 8.95 (s, 1H, OH), 8.60 (s, 1H, NH), 6.69 (d, $J_{5',6'} = 8.0$ Hz, 1H, H-5'), 6.59 (d, $J_{2',6'} = 1.6$ Hz, 1H, H-2'), 6.51 (dd, $J_{6',2'} = 2.0$ Hz, $J_{6',5'} = 6.4$ Hz, 1H, H-6'), 4.71 (s, 1H, H-4), 3.99 (q, $J_{\text{CH}_2,\text{CH}_3} = 6.8$ Hz, 2H, CH₂), 3.65 (s, 3H, OCH₃), 2.40 (d, $J_{\text{H}_a,\text{H}_b} = 16.8$ Hz, 1H, H_a), 2.27 (ovp, 1H, H_b), 2.24 (s, 3H, CH₃), 2.15 (d, $J_{\text{H}_a',\text{H}_b'} = 16.0$ Hz, 1H, H_{a'}), 1.98 (d, $J_{\text{H}_b',\text{H}_a'} = 16.0$ Hz, 1H, H_{b'}), 1.15 (t, $J_{\text{CH}_3,\text{CH}_2} = 6.8$ Hz, 3H, CH₃), 0.99 (s, 3H, CH₃), 0.86 (s, 3H, CH₃); EI-MS m/z (% rel. abund.): 385 (M⁺, 32), 370 (2), 356 (17), 340 (7), 312 (12), 262 (100), 234 (30), 178 (5), 150 (3), 124 (1), 83 (1).

Ethyl-4-(3-bromo-4-hydroxyphenyl)-2,7,7-trimethyl-5-oxo-1,4,5,6,7,8-hexahydroquinoline-3-carboxylate (24)

State: Solid; Color: Light green; Yield: 75 %, M.P.: 148-151 °C; R_f : 0.32 (dichloromethane/methanol, 9.6:0.4); $^1\text{H-NMR}$ (300 MHz, DMSO- d_6): δ_H 9.87 (s, 1H, OH), 9.02 (s, 1H, NH), 7.16 (d, $J_{2',6'} = 1.5$ Hz, 1H, H-2'), 6.93 (d,d, $J_{6',2'} = 1.8$ Hz, $J_{6',5'} = 6.6$ Hz, 1H, H-6'), 6.76 (d, $J_{5',6'} = 8.4$ Hz, 1H, H-5'), 4.70 (s, 1H, H-4), 3.99 (q, $J_{\text{CH}_2,\text{CH}_3} = 6.3$ Hz, 2H, CH₂), 2.43 (d, $J_{\text{H}_a,\text{H}_b} = 17.1$ Hz, 1H, H_a), 2.29 (ovp, 1H, H_b), 2.25 (s, 3H, CH₃), 2.18 (d, $J_{\text{H}_a',\text{H}_b'} = 16.2$ Hz, 1H, H_{a'}), 1.99 (d, $J_{\text{H}_b',\text{H}_a'} = 16.2$ Hz, 1H, H_{b'}), 1.15 (t, $J_{\text{CH}_3,\text{CH}_2} = 7.2$ Hz, 3H, CH₃), 0.99 (s, 3H, CH₃), 0.85 (s, 3H, CH₃); $^{13}\text{C-NMR}$ (75 MHz, DMSO- d_6): δ_C 194.2, 166.7, 151.8, 149.3, 144.8, 140.1, 131.6, 127.5, 115.7, 109.7, 108.3, 103.5, 59.0, 50.1, 39.5, 34.8, 32.1, 29.0, 26.3, 18.2, 14.0; EI-MS m/z (% rel. abund.): 433 (M⁺, 37), 435 (M⁺+2, 26), 406 (11), 365 (17), 322

(14), 273 (29), 262 (100), 252 (13), 234 (66), 217 (5), 197 (5), 178 (11), 150 (5), 115 (3), 83 (16), 43 (21); HREI-MS Calcd for $C_{21}H_{24}O_4N_1Br$: $m/z = 433.0861$, Found 433.0889.

Ethyl-4-(3-(benzyloxy)phenyl)-2,7,7-trimethyl-5-oxo-1,4,5,6,7,8-hexahydroquinoline-3-carboxylate (25) [35]

State: Solid; Color: White; Yield: 50%, M.P.: 140-142 °C; R_f : 0.34 (dichloromethane/methanol, 9.6:0.4); 1H -NMR (400 MHz, DMSO- d_6): δ_H 9.01 (s, 1H, NH), 7.38 (m, 5H, H-2", H-3", H-4", H-5", H-6"), 7.09 (t, $J_{5',4'/5',6'}$ = 7.6 Hz, 1H, H-5'), 6.73 (s, 3H, H-2', H-4', H-6'), 4.98 (s, 2H, CH₂), 4.81 (s, 1H, H-4), 3.98 (q, J_{CH_2,CH_3} = 6.8 Hz, 2H, CH₂), 2.41 (d, J_{H_a,H_b} = 17.2 Hz, 1H, H_a), 2.29 (ovp, 1H, H_b), 2.25 (s, 3H, CH₃), 2.16 (d, $J_{H_a',H_b'}$ = 16.0 Hz, 1H, H_{a'}), 1.98 (d, $J_{H_b',H_a'}$ = 16.0 Hz, 1H, H_{b'}), 1.13 (t, J_{CH_3,CH_2} = 6.8 Hz, 3H, CH₃), 0.99 (s, 3H, CH₃), 0.84 (s, 3H, CH₃); EI-MS m/z (% rel. abund.): 445 (M⁺, 19), 400 (4), 354 (10), 262 (100), 234 (18), 178 (3), 150 (1), 91 (10), 65 (1).

Ethyl-4-(2-(benzyloxy)phenyl)-2,7,7-trimethyl-5-oxo-1,4,5,6,7,8-hexahydroquinoline-3-carboxylate (26)

State: Solid; Color: White; Yield: 60%, M.P.: 146-149 °C; R_f : 0.50 (dichloromethane/methanol, 9.6:0.4); 1H -NMR (400 MHz, DMSO- d_6): δ_H 9.01 (s, 1H, NH), 7.40 (m, 5H, H-2", H-3", H-4", H-5", H-6"), 7.09 (t, $J_{5',4'/5',6'}$ = 8.0 Hz, 1H, H-5'), 6.73 (m, 3H, H-3', H-6'), 4.98 (d, J_{CH_2} = 2.0 Hz, 2H, CH₂), 4.81 (s, 1H, H-4), 3.98 (q, J_{CH_2,CH_3} = 7.2 Hz, 2H, CH₂), 2.41 (d, J_{H_a,H_b} = 17.2 Hz, 1H, H_a), 2.29 (ovp, 1H, H_b), 2.25 (s, 3H, CH₃), 2.16 (d, $J_{H_a',H_b'}$ = 16.0 Hz, 1H, H_{a'}), 1.98 (d, $J_{H_b',H_a'}$ = 15.6 Hz, 1H, H_{b'}), 1.13 (t, J_{CH_3,CH_2} = 7.2 Hz, 3H, CH₃), 0.99 (s, 3H, CH₃), 0.84 (s, 3H, CH₃); EI-MS m/z (% rel. abund.): 445 (M⁺, 17), 372 (2), 352 (10), 324 (1), 262 (100), 234 (18), 177 (4), 91 (2), 65 (3).

Ethyl-4-(3-(benzyloxy)-4-methoxyphenyl)-2,7,7-trimethyl-5-oxo-1,4,5,6,7,8-hexahydroquinoline-3-carboxylate (27)

State: Solid; Color: White; Yield: 60%, M.P.: 150-153 °C; R_f : 0.49 (dichloromethane/methanol, 9.6:0.4); 1H -NMR (400 MHz, DMSO- d_6): δ_H 8.96 (s, 1H, NH), 7.38 (m, 5H, H-2", H-3", H-4", H-5", H-6"), 6.78 (ovp, 2H, H-2', H-5'), 6.66 (d,d, $J_{6',2'}$ = 1.6 Hz, $J_{6',5'}$ = 6.8 Hz, 1H, H-6'), 4.94 (s, 2H, CH₂), 4.75 (s, 1H, H-4), 3.96 (q, J_{CH_2,CH_3} = 3.6 Hz, 2H, CH₂), 3.68 (s, 3H, OCH₃), 2.40 (d, J_{H_a,H_b} = 17.2 Hz, 1H, H_a), 2.27 (ovp, 1H, H_b), 2.23 (s, 3H, CH₃), 2.15 (d, $J_{H_a',H_b'}$ = 16.0 Hz, 1H, H_{a'}), 1.96 (d, $J_{H_b',H_a'}$ = 16.0 Hz, 1H, H_{b'}), 1.13 (t, J_{CH_3,CH_2} = 7.2 Hz, 3H, CH₃), 0.99 (s,

3H, CH₃), 0.84 (s, 3H, CH₃); ¹³C-NMR (75 MHz, DMSO-*d*₆): δ_c 194.7, 167.3, 149.7, 147.7, 147.5, 145.0, 140.8, 137.6, 128.8, 128.2, 128.0, 120.2, 113.9, 112.0, 110.4, 104.1, 70.4, 59.4, 55.9, 50.7, 39.9, 35.4, 32.5, 29.5, 27.0, 18.7, 14.6; EI-MS *m/z* (% rel. abund.): 475 (M⁺, 37), 402 (6), 384 (23), 262 (100), 234 (15), 214 (3), 178 (6), 150 (1), 91 (17), 65 (2). HREI-MS Calcd for C₂₉H₃₃O₅N₁: *m/z* = 475.23472, Found 475.2359.

Ethyl-2,7,7-trimethyl-4-(4-(methylthio)phenyl)-5-oxo-1,4,5,6,7,8-hexahydroquinoline-3-carboxylate (28)

State: Solid; Color: Green; Yield: 59%, M.P.: 174-177 °C; R_f: 0.51 (dichloromethane/methanol, 9.6:0.4); ¹H-NMR (300 MHz, DMSO-*d*₆): δ_H 9.03 (s, 1H, NH), 7.06 (s, 4H, H-2', H-3', H-5', H-6'), 4.78 (s, 1H, H-4), 3.99 (q, $J_{CH_2,CH_3} = 6.9$ Hz, 2H, CH₂), 2.43 (ovp, 1H, 6-H_a) 2.38 (s, 3H, S-CH₃), 2.29 (ovp, 1H, H_b) 2.26 (s, 3H, CH₃), 2.17 (d, $J_{Ha',Hb'} = 16.2$ Hz, 1H, H_{a'}), 1.98 (d, $J_{Hb',Ha'} = 15.9$ Hz, 1H, H_{b'}), 1.14 (t, $J_{CH_3,CH_2} = 7.2$ Hz, 3H, CH₃), 0.99 (s, 3H, CH₃), 0.83 (s, 3H, CH₃); EI-MS *m/z* (% rel. abund.): 385 (M⁺, 95), 356 (34), 312 (23), 262 (100), 252 (24), 234 (56), 227 (14), 178 (14) 150 (7), 83 (6).

Ethyl-4-(4-(dimethylamino)phenyl)-2,7,7-trimethyl-5-oxo-1,4,5,6,7,8-hexahydroquinoline-3-carboxylate (29)

State: Solid; Color: Green; Yield: 56%, M.P.: 193-196 °C; R_f: 0.41 (dichloromethane/methanol, 9.6:0.4); ¹H-NMR (400 MHz, DMSO-*d*₆): δ_H 8.91 (s, 1H, NH), 6.94 (d, $J_{3',2'/5',6'} = 8.8$ Hz, 2H, H-3', H-5'), 6.53 (d, $J_{2',3'/6',5'} = 8.8$ Hz, 2H, H-2', H-6'), 4.71 (s, 1H, H-4), 3.98 (q, $J_{CH_2,CH_3} = 7.2$ Hz, 2H, CH₂), 2.78 (s, 6H, N(CH₃)₂), 2.40 (d, $J_{Ha,Hb} = 17.2$ Hz, 1H, H_a), 2.28 (ovp, 1H, H_b), 2.23 (s, 3H, CH₃), 2.15 (d, $J_{Ha',Hb'} = 16.0$ Hz, 1H, H_{a'}), 1.97 (d, $J_{Hb',Ha'} = 16.0$ Hz, 1H, H_{b'}), 1.15 (t, $J_{CH_3,CH_2} = 7.2$ Hz, 3H, CH₃), 0.99 (s, 3H, CH₃), 0.86 (s, 3H, CH₃); EI-MS *m/z* (% rel. abund.): 382 (M⁺, 100), 367 (13), 353 (35), 337 (15), 309 (91), 298 (12), 262 (89), 252 (4), 234 (24), 205 (7), 189 (15), 178 (9), 150 (3), 121 (27), 105 (6), 77 (4)

Ethyl-2,7,7-trimethyl-4-(4-nitrophenyl)-5-oxo-1,4,5,6,7,8-hexahydroquinoline-3-carboxylate (30) [33]

State: Solid; Color: Green; Yield: 52%, M.P.: 147-149 °C; R_f: 0.47 (dichloromethane/methanol, 9.6:0.4); ¹H-NMR (400 MHz, DMSO-*d*₆): δ_H 9.20 (s, 1H, NH), 8.09 (d, $J_{3',2'/5',6'} = 8.8$ Hz, 2H, H-3', H-5'), 7.41 (d, $J_{2',3'/6',5'} = 8.8$ Hz, 2H, H-2', H-6'), 4.95 (s, 1H, H-4), 3.97 (q, $J_{CH_2,CH_3} = 7.2$ Hz, 2H, CH₂), 2.44 (d, $J_{Ha,Hb} = 17.2$ Hz, 1H, H_a), 2.30 (s, 3H, CH₃), 2.26 (ovp, 1H, H_b), 2.19

(d, $J_{Ha',Hb} = 16.4$ Hz, 1H, H_a'), 1.98 (d, $J_{Hb',Ha'} = 16.0$ Hz, 1H, H_b'), 1.11 (t, $J_{CH_3,CH_2} = 7.2$ Hz, 3H, CH_3), 0.99 (s, 3H, CH_3), 0.80 (s, 3H, CH_3); EI-MS m/z (% rel. abund.): 384 (M^+ , 57), 355 (28), 339 (12), 311 (13), 262 (100), 234 (64), 178 (12), 150 (7), 77 (2)

Ethyl-2,7,7-trimethyl-5-oxo-4-(4-(trifluoromethyl)phenyl)-1,4,5,6,7,8-hexahydroquinoline-3-carboxylate (31)

State: Solid; Color: White; Yield: 55%, M.P.: 179-182°C; R_f : 0.45 (dichloromethane/methanol, 9.6:0.4); 1H -NMR (400 MHz, $DMSO-d_6$): δ_H 9.14 (s, 1H, NH), 7.56 (d, $J_{3',2'/5',6'} = 8.0$ Hz, 2H, H-3', H-5'), 7.35 (d, $J_{2',3'/6',5'} = 8.0$ Hz, 2H, H-2', H-6'), 4.91 (s, 1H, H-4), 3.98 (q, $J_{CH_2,CH_3} = 6.8$ Hz, 2H, CH_2), 2.43 (d, $J_{Ha,Hb} = 16.8$ Hz, 1H, H_a), 2.30 (ovp, 1H, H_b), 2.29 (s, 3H, CH_3), 2.18 (d, $J_{Ha',Hb'} = 16.0$ Hz, 1H, H_a'), 1.98 (d, $J_{Hb',Ha'} = 16.0$ Hz, 1H, H_b'), 1.11 (t, $J_{CH_3,CH_2} = 7.2$ Hz, 3H, CH_3), 0.99 (s, 3H, CH_3), 0.81 (s, 3H, CH_3); EI-MS m/z (% rel. abund.): 407 (M^+ , 21), 378 (13), 362 (10), 334 (7), 262 (100), 234 (34), 178 (6), 149 (3).

References:

1. Davarpanah, J., Ghahremani, M., and Najafi, O. (2019). Synthesis of 1,4-dihydropyridine and polyhydroquinoline derivatives *via* Hantzsch reaction using nicotinic acid as a green and reusable catalyst. *Journal of Molecular Structure*, 1177, 525-535.
2. Bhaskaruni, S. V., Maddila, S., van Zyl, W. E., and Jonnalagadda, S. B. (2018). V_2O_5/ZrO_2 as an efficient reusable catalyst for the facile, green, one-pot synthesis of novel functionalized 1,4-dihydropyridine derivatives. *Catalysis Today*, 309, 276-281.
3. Maleki, A., Firouzi-Haji, R., and Hajizadeh, Z. (2018). Magnetic guanidinylated chitosan nanobiocomposite: A green catalyst for the synthesis of 1,4-dihydropyridines. *International Journal of Biological Macromolecules*, 116, 320-326.
4. Mansoor, S. S., Aswin, K., Logaiya, K., and Sudhan, S. P. N. (2013). Melamine trisulfonic acid as an efficient catalyst for the synthesis of 2,6-dimethyl-4-substituted-1,4-dihydropyridine-3,5-diethyl/dimethylcarboxylate derivatives *via* Hantzsch reaction in solvent free condition. *Journal of King Saud University-Science*, 25(3), 191-199.

5. Ibrahim, S., Al-Ahdal, A., Khedr, A., and Mohamed, G. (2017). Antioxidant α -amylase inhibitors flavonoids from *Iris germanica* rhizomes. *Revista Brasileira de Farmacognosia*, 27(2), 170-174.
6. Lin, M. Z., Chai, W. M., Zheng, Y. L., Huang, Q., and Ou-Yang, C. (2018). Inhibitory kinetics and mechanism of rifampicin on α -glucosidase: Insights from spectroscopic and molecular docking analyses. *International Journal of Biological Macromolecules*, 122 (2019) 1244-1252
7. Taha, M., Javid, M. T., Imran, S., Selvaraj, M., Chigurupati, S., Ullah, H., and Khan, K. M. (2017). Synthesis and study of the α -amylase inhibitory potential of thiadiazole quinoline derivatives. *Bioorganic Chemistry*, 74, 179-186.
8. Santos, C. M., Freitas, M., and Fernandes, E. (2018). A comprehensive review on xanthone derivatives as α -glucosidase inhibitors. *European journal of medicinal chemistry*, 157, 1460-1479.
9. Imran, S., Taha, M., Selvaraj, M., Ismail, N. H., Chigurupati, S., and Mohammad, J. I. (2017). Synthesis and biological evaluation of indole derivatives as α -amylase inhibitor. *Bioorganic Chemistry*, 73, 121-127.
10. Sudan, S. K., Kumar, N., Kaur, I., and Sahni, G. (2018). Production, purification and characterization of raw starch hydrolyzing thermostable acidic α -amylase from hot springs, India. *International Journal of Biological Macromolecules*, 117, 831-839.
11. Han, L., Fang, C., Zhu, R., Peng, Q., Li, D., and Wang, M. (2017). Inhibitory effect of phloretin on α -glucosidase: Kinetics, interaction mechanism and molecular docking. *International Journal of Biological Macromolecules*, 95, 520-527.
12. Zhen, J., Dai, Y., Villani, T., Giurleo, D., Simon, J. E., and Wu, Q. (2017). Synthesis of novel flavonoid alkaloids as α -glucosidase inhibitors. *Bioorganic and Medicinal Chemistry*, 25(20), 5355-5364.
13. Gollapalli, M., Taha, M., Ullah, H., Nawaz, M., AlMuqarrabun, L. M. R., Rahim, F., and Khan, K. M. (2018). Synthesis of *Bis*-indolylmethane sulfonylhydrazides derivatives as potent α -Glucosidase inhibitors. *Bioorganic Chemistry*, 80, 112-120.

14. Peng, X., Zhang, G., Liao, Y., and Gong, D. (2016). Inhibitory kinetics and mechanism of kaempferol on α -glucosidase. *Food Chemistry*, 190, 207-215.
15. Taha, M., Imran, S., Ismail, N. H., Selvaraj, M., Rahim, F., Chigurupati, S., and Vijayabalan, S. (2017). Biology-oriented drug synthesis (BIO DS) of 2-(2-methyl-5-nitro-1*H*-imidazol-1-yl) ethyl aryl ether derivatives, *in vitro* α -amylase inhibitory activity and *in silico* studies. *Bioorganic Chemistry*, 74, 1-9.
16. Khan, M., Alam, A., Khan, K. M., Salar, U., Chigurupati, S., Wadood, A., and Perveen, S. (2018). Flurbiprofen derivatives as novel α -amylase inhibitors: Biology-oriented drug synthesis (BIO DS), *in vitro*, and *in silico* evaluation. *Bioorganic Chemistry*, 81, 157-167.
17. Hameed, A., Anwar, A., Yousaf, S., Khan, K. M., and Basha, F. Z. (2012). Urease inhibition and anticancer activity of novel polyfunctional 5,6-dihydropyridine derivatives and their structure-activity relationship. *European Journal of Chemistry*, 3, 179-185.
18. Niaz, H., Kashtoh, H., Khan, J. A., Khan, A., Alam, M. T., Khan, K. M., and Choudhary, M. I. (2015). Synthesis of diethyl 4-substituted-2,6-dimethyl-1,4-dihydropyridine-3,5-dicarboxylates as a new series of inhibitors against yeast α -glucosidase. *European Journal of Medicinal Chemistry*, 95, 199-209.
19. Mansoor, S. S., Aswin, K., Logaiya, K., and Sudhan, S. P. N. (2016). Bismuth nitrate as an efficient recyclable catalyst for the one-pot multi component synthesis of 1,4-dihydropyridine derivatives through unsymmetrical Hantzsch reaction. *Journal of Saudi Chemical Society*, 20, S100-S108.
20. Tekale, S. U., Pagore, V. P., Kauthale, S. S., and Pawar, R. P. (2014). La₂O₃/TFE: An efficient system for room temperature synthesis of Hantzsch polyhydroquinolines. *Chinese Chemical Letters*, 25(8), 1149-1152.
21. Evans, C. G., and Gestwicki, J. E. (2009). Enantioselective organocatalytic Hantzsch synthesis of polyhydroquinolines. *Organic Letters*, 11(14), 2957-2959.
22. Paidepala, H., Nagendra, S., Saddanappu, V., Addlagatta, A., and Das, B. (2014). Catalyst-free efficient synthesis of polyhydroquinolines using polyethylene glycol as a

- solvent and evaluation of their cytotoxicity. *Medicinal Chemistry Research*, 23(2), 1031-1036.
23. Lambat, T., Deo, S., and Deshmukh, T. (2014). Sulphamic acid assisted synthesis of polyhydroquinolines via Hantzsch multicomponent reaction: a green approach. *Journal of Chemical Pharmaceutical Research*, 6(4), 888-892.
24. Reddy, M. V., and Jeong, Y. T. (2012). Polystyrene-supported *p*-toluenesulfonic acid: A new, highly efficient, and recyclable catalyst for the synthesis of hydropyridine derivatives under solvent-free conditions. *Synlett*, 23(20), 2985-2991.
25. Norouzi, M., Ghorbani-Choghamarani, A., Nikoorazm, M. (2016). Heterogeneous Cu(II)/1-His₂Fe₃O₄ nanocatalyst: a novel, efficient and magnetically-recoverable catalyst for organic transformations in green solvents. *RSC Advances*, 6(95), 92387-92401.
26. Zolfigol, M. A., Baghery, S., Moosavi-Zare, A. R., Vahdat, S. M., Alinezhad, H., and Norouzi, M. (2014). Synthesis of the first nano ionic liquid 1-methylimidazolium trinitromethanide {[HMIM]C(NO₂)₃} and its catalytic use for Hantzsch four-component condensation. *RSC Advances*, 4(101), 57662-57670.
27. Xiong, X., Yi, C., Liao, X., Lai, S. (2019). An Effective One-Pot Access to 2-Amino-4*H*-benzo[*b*]pyrans and 1,4-Dihydropyridines via γ -Cyclodextrin-Catalyzed Multi-Component Tandem Reactions in Deep Eutectic Solvent. *Catalysis Letters*, 149(6), 1690-1700.
28. Khaligh, N. G. Four-component one-pot synthesis of unsymmetrical polyhydroquinoline derivatives using 3-methyl-1-sulfonic acid imidazolium hydrogen sulfate as a catalyst. *Chinese Journal of Catalysis*, 35(7), 1036-1042.
29. Vahdat, S. M., Zolfigol, M. A., and Baghery, S. (2016). Straightforward Hantzsch four- and threecomponent condensation in the presence of triphenyl(propyl-3-sulfonyl) phosphoniumtrifluoromethanesulfonate {[TPPSP]OTf} as a reusable and green mild ionic liquid catalyst. *Applied Organometallic Chemistry*, 30, 311-317

30. Kulkarni, P. (2013). $\text{Al}_2(\text{SO}_4)_3$ is an efficient and mild acid catalyst for the one-pot, four-component synthesis of polyhydroquinoline. The 17th International Electronic Conference on Synthetic Organic Chemistry.
31. Choghamarani, A. G., Moradi, P., Tahmasbi, B. (2018). Nickel(II) immobilized on dithizone-boehmite nanoparticles: as a highly efficient and recyclable nanocatalyst for the synthesis of polyhydroquinolines and sulfoxidation reaction. *Journal of the Iranian Chemical Society*, 16(3), 511-521.
32. Vijaykumar, J. M., and Rajendra, P. P. (2013). Microwave-assisted expeditious synthesis of bioactive polyhydroquinoline derivatives. *European Chemical Bulletin*, 2(9), 679-682.
33. Zarchi, M. A. K., Abadi, S. S. A. D. M. (2016). Facile and efficient protocols for C-C and C-N bond formation reactions using a superparamagnetic palladium complex as reusable catalyst. *Research on Chemical Intermediates*, <https://doi.org/10.1007/s11164-019-03754-y>.
34. Paidepala, H., Nagendra, S., Saddanappu, V., Addlagatta, A., Das, B. (2014). Catalyst-free efficient synthesis of polyhydroquinolines using polyethylene glycol as a solvent and evaluation of their cytotoxicity. *Medicinal Chemistry Research*, 23, 1031-1036.
35. Perumal, M., Sengodu, P., Venkatesan, S., Perumal, S., Antony, S., Paramsivam, M. (2017). Polybenzimidazole-triphenylphosphene-catalyzed one-pot synthesis and evaluation of dihydropyridine derivative as antibiotics and antifungals. *Chemistry Select*, 2, 7489-7496.

Dihydropyridines as potential α -Amylase and α -Glucosidase Inhibitors: Synthesis, *In Vitro* and *In Silico* Studies

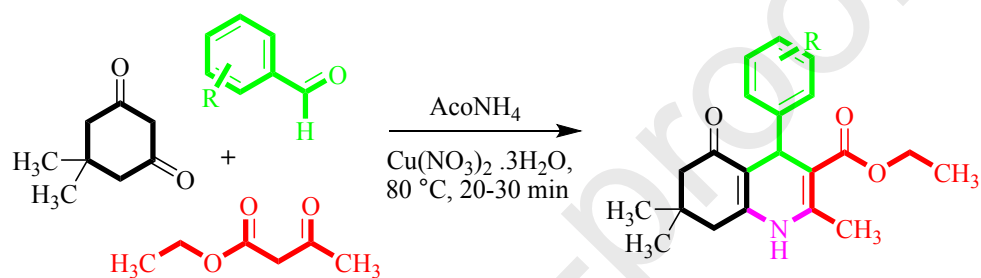
Hina Yousuf,^a Shahbaz Shamim,^a Khalid Mohammed Khan,^{a,b} Sridevi Chigurupati,^c Kanwal,^a Shehryar Hameed,^a Muhammad Naseem Khan,^d Muhammad Taha,^b Minhajul Arfeen^c

^aH. E. J. Research Institute of Chemistry, International Center for Chemical and Biological Sciences, University of Karachi, Karachi, 75270, Pakistan

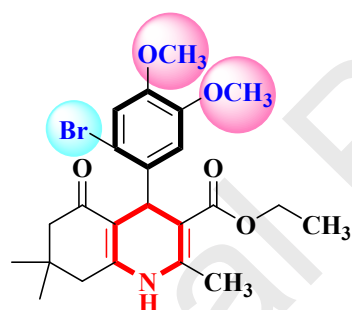
^bDepartment of Clinical Pharmacy, Institute for Research and Medical Consultations (IRMC), Imam Abdulrahman Bin Faisal University, P.O. Box 1982, Dammam, 31441, Saudi Arabia

^cDepartment of Medicinal Chemistry and Pharmacognosy, College of Pharmacy, Qassim University, Buraidah, 52571, Saudi Arabia

^dDepartment of Chemistry, COMSATS University Islamabad, Abbottabad campus, Abbottabad (22010) Pakistan



A

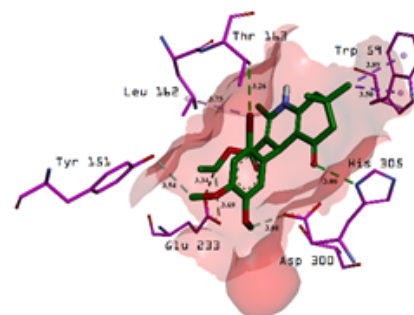


18

α -Amylase Inhibition
 $IC_{50} = 2.31 \pm 0.09 \mu M$

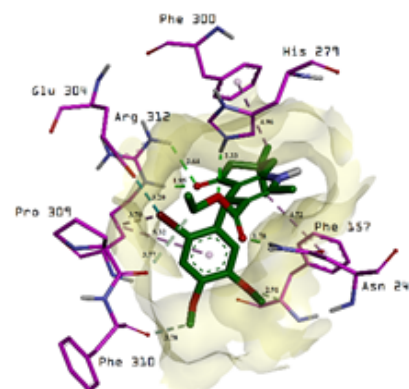
α -Glucosidase Inhibition
 $IC_{50} = 2.21 \pm 0.06 \mu M$

Dual Inhibitor



Docked conformation of synthesized compounds with the side chain residues of α -amylase, Ligands shown in green color, side chain amino acids in violet color, and distances (Angstrom) colored in black; A) Interactions of compound 18

A



Docked conformation of synthesized compounds with the side chain residues of α -glucosidase, Ligands shown in green color, side chain amino acids in violet color, and distances (Angstrom) colored in black; A) Interactions of compound 18

Conflict of Interest

The authors declare to have no conflict of interest.

Journal Pre-proofs

Highlights

- Dihydropyridines (**1-31**) were designed and synthesized.
- The synthetic molecules were screened for α -amylase and α -glucosidase inhibitory activities.
- Limited structure-activity relationship was developed based on the different substituent patterns on aryl part.
- *In silico* studies were performed to confirm the binding interactions of synthetic molecules with the enzyme active site.
- This study had identified potential urease inhibitors which can be used as lead molecules for further studies.